Photocapacitance Measurement of Deep Levels in GaAs

By

Muhammad Yaqoob

Department of Physics
Quaid-i-Azam University
Islamabad, Pakistan.
2011

In the name of almighty Allah, the most Gracious, the most Merciful.

This work is submitted as a dissertation in partial fulfillment for the award of the degree of

MASTER OF PHILOSOPHY

In

PHYSICS

Department of Physics
Quaid-i-Azam University
Islamabad, Pakistan.
2011

Certificate

It is certified that the work contained in this dissertation is carried out and completed under my supervision at department of physics, Quaid-i-Azam University, Islamabad, Pakistan.

Supervised by:

(Dr. Umar Saeed Qurashi)
Assistant Professor
Quaid-i-Azam
University
Islamabad,Pakistan.

Submitted through:

(Prof. Dr. S.K Hasanain)
Chairman
Department of Physics
Quaid-i-Azam University
Islamabad, Pakistan.

To

My family

Acknowledgements

I am filled with the praise and glory to All Mighty Allah, the most merciful and benevolent, Who created the universe, with ideas of beauty, symmetry and harmony, with regularity and without any chaos, and gave us the abilities to discover what he thought.

Bless Muhammad (P. B. U. H) the seal of the prophets, and his pure and pious progeny.

First and the foremost, I want to express my deepest gratitude to my venerable teacher and supervisor, ***Dr. Umar Saeed Qureshi*** *for his worthy kindness and invaluable favors. He guided my work with infinite patience, enthusiasm and a great amount of tolerance. With all my ventures, I always could rely on his remarkable ability to quickly distill any problem to its essence.*

I am thankful to ***Chairman, Dr. S. K. Hasanain*** *for supporting and encouraging me throughout my research work.*

I would like to thanks my senior miss Aqdas for helping me during my DLTS experiment. I would like to thank my Lab fellows Rashid, Waqas, Zafar and Sehrish for providing me a cooperative environment in the Lab. My cordial thanks to my friends Ashiq, Naseem, Munir, Rashid, Mehar and Shoaib, Their warm companionship make the life at campus beautiful and unforgetable.

I can never thank enough my parents for everything they have done for me. Even then, I wish to record my deepest obligations to my father and my brother who always loves and support me and my mother and grandmother for her endless contribution to make me stay on the track. No one tolerates me more than they do. I am forever indebted to the love and caring of my sisters. A great thanks to my family for their unconditional support, belief in me and for keeping me grounded.

Muhammad Yaqoob

Abstract

Photocapacitance technique for the measuring electron and hole photoionization cross-section has been developed and setup. Deep levels in p-type GaAs, drown by metal organic chemical vapor deposition (MOCVD) has been investigated through this technique. Photocapacitance experiments were performed at two different temperatures (room temperature and 80K) by using the initial condition (switching bias from 0 to 3V). DLTS revealed that presence of majority level having activation energy 0.54eV. This level is identified as the HM1 defect in p-type GaAs. This defect level is corresponds to the well known EL2 defect in n-type GaAs.

This technique has been used to measure the photoionization cross-section (σ_n° + σ_p°) for the HM1 level at different photon energies. The transformation of EL2 to metastable level has been achieved through photo-quenching experiment. The spectra distribution of this transformation has been measured.

LIST OF CONTENTS

CHAPTER 1

INTRODUCTION

1.1 Essence of Semiconductors

A semiconductor can be considered as a material having conductivity ranging between that of an insulator and a metal. A crucial property of semiconductors is the band gap, a range of forbidden energies within the electronic structure of the material. Semiconductors typically have band gaps ranging between 1 and 4 eV, while insulators have larger band gaps, often greater than 5 eV [1]. The thermal energy available at room temperature, 300 K, is approximately 25 meV and is thus considerably smaller than the energy required to promote an electron across the band gap. This means that there are a small number of carriers present at room temperature, due to the high energy tail of the Boltzmann-like thermal energy distribution. However this number can be changed by introducing of shallow defects (e.g. P or B in Si). It is the ability to control the number of charge carriers that makes semiconductors of great technological importance. Semiconducting materials are very sensitive to impurities in the crystal lattice as these can have a dramatic effect on the number of mobile charge carriers present. The controlled addition of these impurities is known as doping and allows the tuning of the electronic properties, an important requirement for technological applications. The properties of a pure semiconductor are called 'intrinsic', whilst those resulting from the introduction of dopants are called 'extrinsic'. This introduction of dopants results in the creation of new, intra-band, energy levels and the generation of either negative (electrons) or positive (holes) charge carriers.

1.1.1 Semiconductor Materials.

The semiconductor technology is only half a century old, but its introduction brought a revolution in electronic engineering, starting with the invention of bipolar transistor by W.Shockley, J.Bardeen and W. Brattain in 1951 [2], and since then it has

flourished extremely fast and still does. The semiconductor devices are getting faster, smaller, cheaper and new ones are constantly being developed.

The materials most often used in semiconductor devices are germanium and silicon. Germanium has higher electrical conductivity (less resistance to current flow) than silicon, and is used in most low– and medium–power diodes and transistors. Silicon is more suitable for high–power devices than germanium. One reason is that it can be used at much higher temperatures. The wide band gap III-V nitrides have long been recognized as materials of outstanding optical, electronics and thermal properties [3]. A relatively new material which combines the principal desirable features of both germanium and silicon is gallium arsenide. When further experience with this material has been obtained, it is expected to find much wider use in semiconductor devices. In optoelectronics, compounds originating from III-V in the periodic table (called III-Vs) such as InGaAs, AlGaAs and InP are better suited due to their higher recombination efficiency. For application in the near UV region of spectrum, III-V nitrides such as GaN, InGaN show promising properties [4]. Artificially tailored semiconductor hetrostructures now form the leading edge of the device technology. By alternating thin layers of e.g.GaAs with e.g. (AlGa)As, one can produce structure with remarkable optoelectronics properties, such as high quality, low dimensions electronic structures like 'Quantum Well , 'Quantum Wires' , 'Quantum Dots' based layers and many others. They are fabricated by techniques such as molecular beam epitaxy (MBE) [5] and metal organic chemical vapor deposition (MOCVD)[6] and can be patterned using optical or electron based lithography techniques to form real devices which opens up a new field of basic research and lead to a wealth of novel application.

1.1.2 III-V Semiconductors

III-V compound semiconductors are wide band-gap materials commonly used for optoelectronics devices. Most of III-V semiconductors are direct band-gap but some material have indirect band-gap. The direct band-gap materials are suitable for optoelectronics applications. In direct band-gap material both the photon emission and absorption can occur without any involvement of lattice phonon to conserve momentum,

therefore, the radiative recombination efficiencies of these materials are much higher as compared to the indirect band-gap materials, but the life time of the direct band-gap materials are generally smaller than indirect band-gap. The band gap of III-V semiconductor compounds can be varied by varying the percentage of one of the compounds. Thus a continuous band-gap variation can be possible. (Fig.1.1).

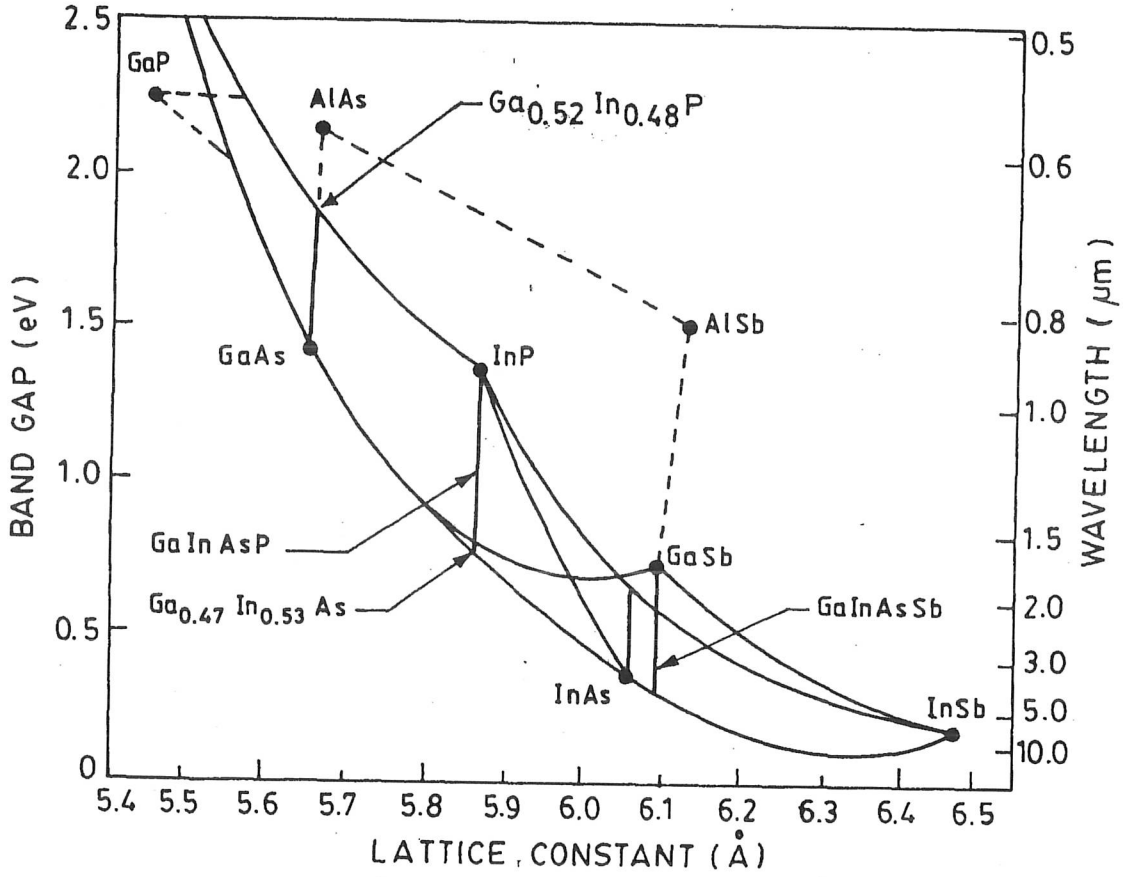

Figure 1.1: Energy gap versus lattice constant for III-V compound semiconductor

Importance of III-V semiconductors

1 III-V semiconductors are wide band-gap materials commonly used as optoelectronics devices such as LASERS. LEDs and Gunn diodes.

2. The interesting property that has made them attractive is the formation of ternary compounds using MBE and MOCVD techniques.

3. BN (cubic) has indirect band gap and BN (Hexagonal) has quasi-direct band-gap, they are potentially useful for ultraviolet LEDs.

4. BAs and B12As2 have direct band-gap, are resistant to radiation damage and have possible applications in betavoltaics.

5. GaSb used for infrared detectors and LEDs and thermophotovoltaics.

6. The compound GaAs, second most common in use after silicon, commonly used as substrate for other III-V semiconductors, e.g. InGaAs and GaInNAs. It has many more qualities like high impurity density, difficult to fabricate small structures. Used for near-IR LEDs, fast electronics, and high-efficiency solar cells, very similar lattice constant to germanium, can be grown on germanium substrates. Also used in solar technology.

7. III-V semiconductors compounds are used in space and military applications due to higher radiation hardness and are capable of operating over a wide temperature range (-196 to 300 C).

8. GaN is suitable for spacecraft solar panels as it is insensitive to ionizing radiation. GaN transistors can operate at higher voltages and higher temperatures than GaAs, used in microwave power amplifiers. When doped with e.g. manganese, becomes a magnetic semiconductor.

9. InN has possible use in solar cells.

10. GaAsP is used in red, orange and yellow LEDs.

11. InP is used in high-power and high-frequency applications and also used in solar cell technology.

12. The interest of III-V has increased due to MOCVD and MBE growth techniques which allow the fine tuned variability of boundary conditions and thus permits the stoichiometric growth of compound semiconductors. Using these techniques one can grow structures like quantum well. Quantum dots, quantum lines, high electron mobility transistors etc.

1.1.4 Gallium Arsenide (GaAs).

Gallium Arsenide (GaAs) is a compound of the elements Gallium (Ga) and arsenic (As). It is a III-V semiconductor compound. It is used to make devices, such as microwave frequency integrated circuits, infrared light emitting diodes, laser diodes and solar cells.

Gallium arsenide, a direct band-gap semiconductor, has long appeared to be the most promising of the III–V compounds for device applications. Perhaps because of this, it is also one of the most studied.

In the compound, gallium has a +3 oxidation state. Gallium arsenide can be prepared by direct reaction from the elements which is used in a number of industrial processes [7], e.g. crystal growth using a horizontal zone furnace in the Bridgman-Stockbarger technique, in which gallium and arsenic vapors react and free molecules deposit on a seed crystal at the cooler end of the furnace.

1.1.5 Properties of Gallium Arsenide (GaAs).

- GaAs has some electronic properties which are superior to those of silicon. It has a higher saturated electron velocity and higher electron mobility, allowing transistors made from it to function at frequencies in excess of 250 GHz.

- Unlike silicon junctions, GaAs devices are relatively insensitive to heat due to their higher band-gap also GaAs device tend to have less noise than silicon devices especially at high frequency due to higher carrier mobilities and lower resistive device parasitic. These properties recommend GaAs circuitry in mobile phones, satellite communications and higher frequency radar system.

- Crystal structure: GaAs has a cubic (zinc blend) structure in which the coordinates have fourfold tetrahedral symmetry: that is, each ion, gallium or arsenide is symmetrically surrounded by four ions of further element, each located at the corner of regular tetrahedral. GaAs crystal contain repeated face centered cubic (f.c.c) sub lattices of one type of atom (As) of cube edge length a= 0.56533 nm (5.6533 A) interpenetrating a similar f.c.c sub lattice of identical cube-edge length composed entirely of second type of atoms (Ga). The arsenic sub lattice is displaced by vector (a/4,a/4,a/4) with respect to gallium sub lattice (0, 0, 0). At room temperature and atmospheric pressure, the distance between nearest neighbor Ga-As pair is 0.245. (Fig 1.2)

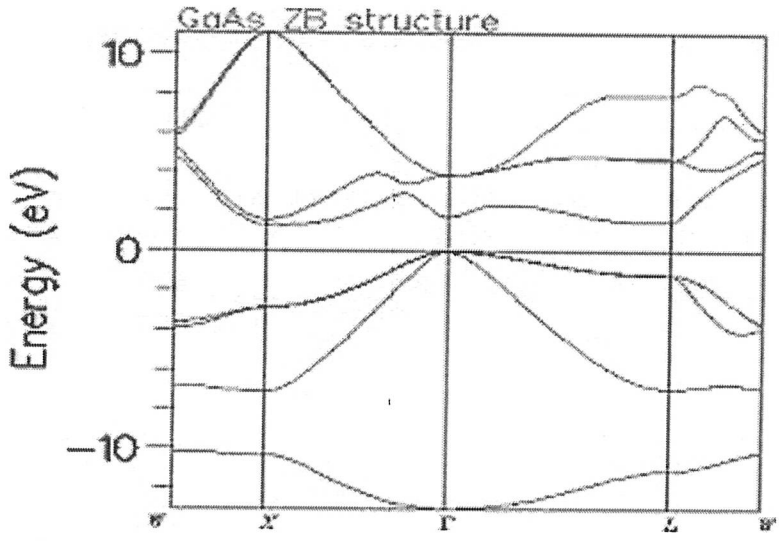

Figure 1.2: Band structure of Gallium Arsenide.

- Another advantage of GaAs is that it has a direct band gap, which means that it can be used to emit light efficiently. Silicon has an indirect band-gap and so is very poor at emitting light. Nonetheless, recent advances may make silicon LEDs and lasers possible. Due to its lower band-gap though, Si LEDs can not emit visible light and rather work in IR range while GaAs LEDs function in visible red light.

- Because of its wide band-gap, pure GaAs is highly resistive. Combined with the high dielectric constant, this property makes GaAs a very good electrical substrate and unlike Si provides natural isolation between devices and circuits. This has made it an ideal material for microwave and millimeter wave integrated circuits, MMICs, where active and essential passive components can readily be produced on a single slice of GaAs.

- One of the first GaAs microprocessors was developed in the early 1980s by the RCA corporation and was considered for the Star Wars program of the United States Department of Defense. Those processors were several times faster and several orders of magnitude more radiation hard than silicon counterparts, but they were rather expensive [8].

- Complex layered structures of gallium arsenide in combination with aluminum arsenide (AlAs) or the alloy AlxGa1-xAs can be grown using molecular beam epitaxy (MBE) or using metalorganic vapor phase epitaxy (MOVPE). Because GaAs and AlAs have almost the same lattice constant, the layers have very little induced strain, which allows them to be grown almost arbitrarily thick. This allows for extremely high performance high electron mobility, HEMT transistors and other quantum well devices.

1.2 Metal Organic Chemical Vapor Deposition (MOCVD).

III - V materials are typically mainly produced by Liquid Phase Epitaxy (LPE), Molecular Beam Epitaxy (MBE) and Metal Organic Chemical Vapor Deposition (MOCVD). The MOCVD process, which was first described by Manasevit, [9] is a very

complex process and the deposition of high quality material films requires the full understanding and control of various chemical and physical processes both in the gas phase and on the surface of the substrate. It has become an important technique in the epitaxy of III-V semiconductor compounds because of its versatility, reproductibility, and large scale production of epitaxial films with satisfactory quality.

In the field of III-V materials, the MOCVD process is preferably used for the deposition of thin material films of the light homologues of group V elements, N, P and As (e.g. GaN, InP, GaAs). In contrast, the deposition procedure of the corresponding antimonides, which find interesting applications in optoelectronic devices (photo detectors, LEDs, lasers) and thermophotovoltaics (GaSb) [10].

The reaction used for the growth of compound semiconductors MOCVD layers is given in the general form

$$RnM + XHn \longrightarrow MX + nRH$$

Where

'R' is an Organic Radical, 'M' is one compound of resulting semiconductor layer, 'X' is other component, and 'n' is an integer.

1.3 Motivation

Photocapacitance is a very sensitive technique and it provides the information about the deep levels I semiconductor martial. This information is used for determination of optical threshold energies. Beside the spectral dependence of the photoionization cross-section of deep level centers, which are directly proportional to optical emission rates, also can be determined by using photpcapacitance technique.

In the semiconductor physics laboratory, the experimental setup for the photocapacitance measurements was not well established. The basic unit such reliable capacitance meter, temperature controller, cryostat, x-t recorder, light source and monochromator with numerous accessories already exists in the laboratory. These unit were assemble together

to established the photocapacitance technique. This formed the major motivation for this work.

After reassembling this technique it was used in semiconductor physics Lab for the characterization of HM1 defect in p –type GaAs.

Thus the purpose work was two-fold: first, reassembling of an experiment set-up photociacitance and photoionization technique in semiconductor physics Lab. Secondly using this technique to study the properties of deep level in p-GaAs, such as photoionization cross-section and quenching.

1.4 Reference

1. H. P. Myers, Introductory Solid State Physics, Taylor & Francis, 1990
2. W. Shokley, circuit element utilizing semiconductor materials, US patent 2569347, 1551.
3. Lung-Hang Peng, C.-M.Lai, C.-W.Shih, C.-C.Chuo and J-I.Chyi(2003).
4. H. Morkoc, F. Hamdani and A.Salvador, electronics and optical properties of III-V nitrides based quantum wells and super lattice, in semiconductors and semimetals, VOL 50, Chap.08 Pp193-257 (1998).
5. Jaeger, Richard C. (2002). "Film Deposition". Introduction to Microelectronic Fabrication. Upper Saddle River: Prentice Hall.
6. G. B. Stringfellow in Organometallic Vapor-Phase Epitaxy: Theory and Practice, Academic Press, Boston, MA (1989)
7. S. J. Moss, A. Ledwith (1987). The Chemistry of the Semiconductor Industry. Springer.
8. Von Jurij Šilc, Borut Robič, Theo Ungerer (1999). Processor architecture: from dataflow to superscalar and beyond. Springer.
9. H. M. Manasevit, Appl. Phys. Lett. (1968.)
10. M. Razeghi, Eur. Phys. J. Appl. Phys. 2003, 23, 149.

Chapter 2

DEEP LEVEL DEFECTS IN SEMICONDUCTORS

This chapter explains the type of defects, theory of deep level kinetics in view of Shockley-Read-Hall statistics and different characterization parameters that are usually used to describe the deep level.

2.1 Defect characteristics

An imperfection of the crystal structure is normally referred to as a defect. The microscopic structure of a defect can be very different. Native defects are formed by missing atoms or excess host atoms. Rows or planes of these defects form dislocations and play a significant role in affecting the mechanical, electrical and optical properties of crystals.

Point defects such as a vacancy or a foreign atom may affect the electronic state of the crystal and often resulting in energy levels within the band gap. A large class of defects originates from elemental impurities, introduced either during the crystal growth or by later processing, deliberately or accidental. The impurities have different effects on the electrical properties of the semiconductor material, depending on the basic defect features such as ionization energy and capture rate of free carriers.

The defect atom can be located in several different positions in the crystal structure. A crystal host atom replaced by the defect atom is referred to as a substitutional impurity. Defect atoms can occupy irregular sites, so called interstitial positions in the space between the host atoms. The energetically most favorable sites are often those exhibiting high symmetry, e.g. tetrahedral symmetry. Depending on the details of the binding mechanism and lattice distortion, though, other sites may occur.

Traditionally, a distinction is made between energetically shallow and deep defect levels. In silicon, a shallow level has ionization energy of less than about 50meV and levels exhibiting higher ionization energies are regarded as deep. A more stringent definition is based on the resemblance of a shallow defect level with the hydrogen atom

regarding its electronic states in the crystal, where the permeability and effective masses are those of the crystal, the Effective Mass Theory (EMT). **[1]** If the energy positions of the electronic states arising from the defect are satisfactory described by this model the defect is said to be shallow, otherwise it is regarded as a deep level.

These structural defects and impurities introduce energy states often in the forbidden gap of the semiconductor. According to the positions of these levels in the band gap with respect to conduction or valence band edge, defects in semiconductors normally place into two categories:

-Shallow level defects
-Deep level defects.

These two groups of defects in semiconductor material play a particular role in the formation of electronic devices fabricated from the material containing them.

2.1.1 Shallow Level Defects

The energy level within the forbidden gap having small binding energies (typically<<0.1eV) are termed as shallow levels **[2].** Shallow levels in the band gap are electrically active, and act as either donors or acceptors and contribute electrons or holes respectively. The associated wave function of such defects is not localized, that is why can be described as hydrogen like defect. They determine the conduction properties of semiconductors and are almost fully ionized at room temperature. Impurities from column III and column V of the periodic table when introduced into column IV elements usually lea to energy levels closed to the valence and conduction band edges.

2.1.2 Deep Level Defects

Deep level effects bind the carrier more strongly than shallow level and lead to highly localized in the band gap, and energy require ionize them is several kT. Deep level can not be described by hydrogenic effective mass theory. They are commonly caused by the impurities, device processing steps and irradiation with the high energy

particles. For example, impurities from columns other than III and V of periodic table such as copper and gold etc. introduce energy level nearer to the middle of the forbidden energy gap. Deep level defects have enormous impact on the performance of the electronic device and play a key role in controlling the minority carrier lifetime.

2.2 The Role of Deep Levels in Semiconductors

The importance of deep level arises from the fundamental role they can play in semiconductor materials. It is well known that deep level centers can act as recombination, generation or trap centers under different conditions are illustrated in fig 2.1. They are "deep" in the sense that the energy require to remove an electron or hole from the trap to the valence or conduction band is much larger than the characteristic thermal energy kT. Deep traps interfere with more useful types of doping by compensating the dominant charge carrier type, annihilating either free electrons or electron holes depending on which is more prevalent. They also directly interfere with the operation of transistors, light-emitting diodes and other electronic and opto-electronic devices, by offering an intermediate state inside the band gap. Deep-level traps shorten the non-radiative life time of charge carriers, and promote recombination of minority carriers, having adverse effects on the semiconductor device performance. This reduction of carrier-lifetime is major cause of degradation of energy conversion efficiency of silicon single crystal solar cells during upper space application. Deep level defect may increase the leakage current of the device and also deteriorate the efficiency if LEDs.

2.3 Shockley-Read-Hall Statistics

The Shockley-Read-Hall (SRH) model was introduced in 1952, **[2] [3]** to describe the statistics of recombination and generation of holes and electrons in semiconductors occurring through the mechanism of trapping. **[4]**

Band diagrams of perfect single crystal semiconductor consist of valence band and conduction and separated by band gap. When the periodicity of a single crystal is perturbed by foreign atom or crystal defects, discrete energy level s are introduce into band gap, shown by E_T lines in figure 2.1.

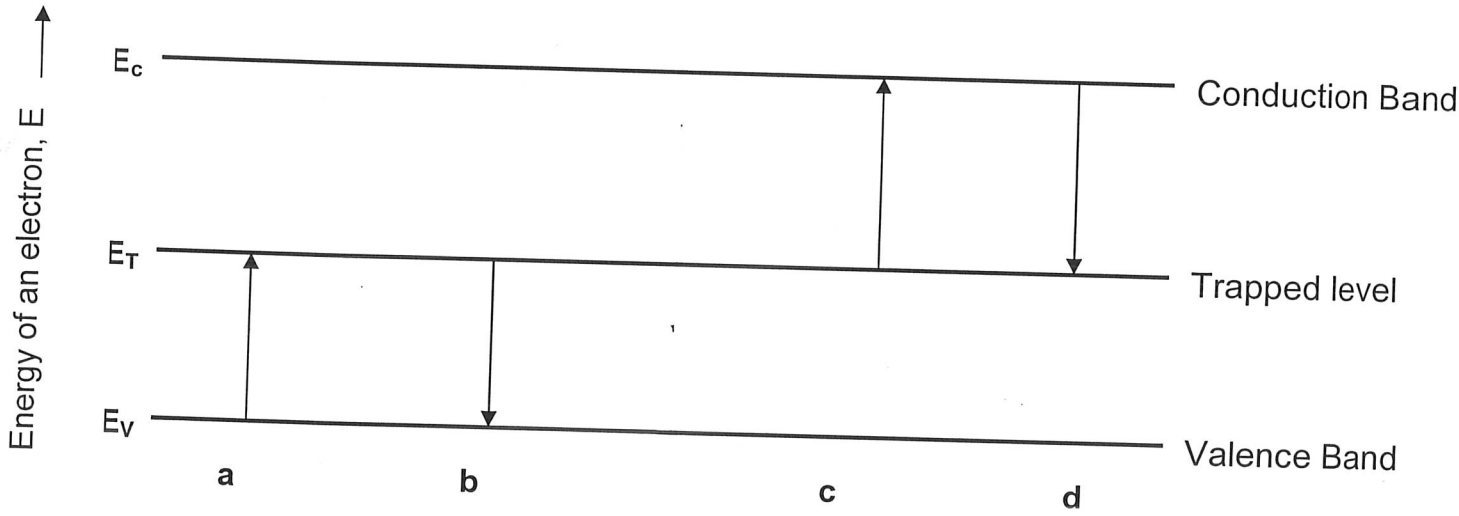

Fig 2.1: ***The four basic processes of electron-hole recombination.***

The transfer of electrons from the valence band to the conduction band is referred to as the generation of electron-hole pairs (or pair-generation process), since not only a free electron is created in the conduction band, but also a hole in the valence band which can contribute to the charge current. The inverse process is termed recombination of electron-hole pairs. The band gap between the upper edge of the valence band and the lower edge of the conduction band is very large in semiconductors, which means that a big amount of energy is needed for a direct band-to-band generation event. The presence of trap levels within the forbidden band caused by crystal impurities facilitates this process, since the jump can be split into two parts, each of them 'cheaper' in terms of energy. The basic mechanisms are illustrated in figure 2.1

(a) Hole emission (an electron jumps from the valence band to the trapped level),

(b) Hole capture (an electron moves from an occupied trap to the valence band, a hole disappears),

(c) Electron emission (an electron jumps from trapped level to the conduction band),

(d) Electron capture (an electron moves from the conduction band to an unoccupied trap).

The concentration of unoccupied centers is given by $N_T(1-f)$, where N_T is the concentration of trap and 'f' is the Fermi-Dirac distribution function, designates the probability of occupation of center by an electron given by

$$f = \frac{1}{1 + \exp \frac{E_T - E_F}{kT}}$$

Where E_T is the energy position of the center, E_F is the Fermi energy position, k is the Boltzmann constant and T is the absolute temperature.

The rate of hole-emission, process (a) is given by

$$R_a = e_p N_T (1 - f) \qquad (2.1)$$

Similarly the rate of hole capture process, process (b) is given by

$$R_b = c_p pNf$$

Or

$$R_b = \sigma_p \langle v_{th} \rangle pNf \qquad (2.2)$$

Where σ_p, e_p and p are hole capture cross-section, hole probability and hole concentration in the valence band, respectively.

The rate of electron emission process (c), proportional to the concentration of occupied centers '$N_T f$' is given by

$$R_c = e_n N_T f \qquad (2.3)$$

The proportionality constant 'e_n' is called electron emission probability.

Similarly the electron capture process (d) is given by

$$R_d = c_n n N_T (1 - f) \qquad (2.4)$$

The proportionality constant $cn = \sigma_n \langle V_{th} \rangle$ is the electron capture coefficient, where σ_n is the electron capture cross-section of trap and $<V_{th}>$ is the average thermal velocity of electrons. Thus the rate of change of filled trap centers n_T is given by

$$\frac{dn_T}{dt} = R_d - R_c - R_b + R_a \qquad (2.5)$$

The following equations gives the rate of change of electron concentration and rate of change of hole concentration respectively

$$\frac{dn}{dt} = R_d - R_c \qquad (2.6)$$

$$\frac{dp}{dt} = R_b - R_a \qquad (2.7)$$

Under equilibrium condition $\frac{dn}{dt} = 0$

From equation (2.6) $R_c = R_d$ *(Detailed Balance Principle)*

i.e. the electron emission and capture rates are equal.

Now we consider the non-equilibrium of semiconductor in which the material is, for instance, uniformly illuminated with the uniform generation rate G per unit volume.

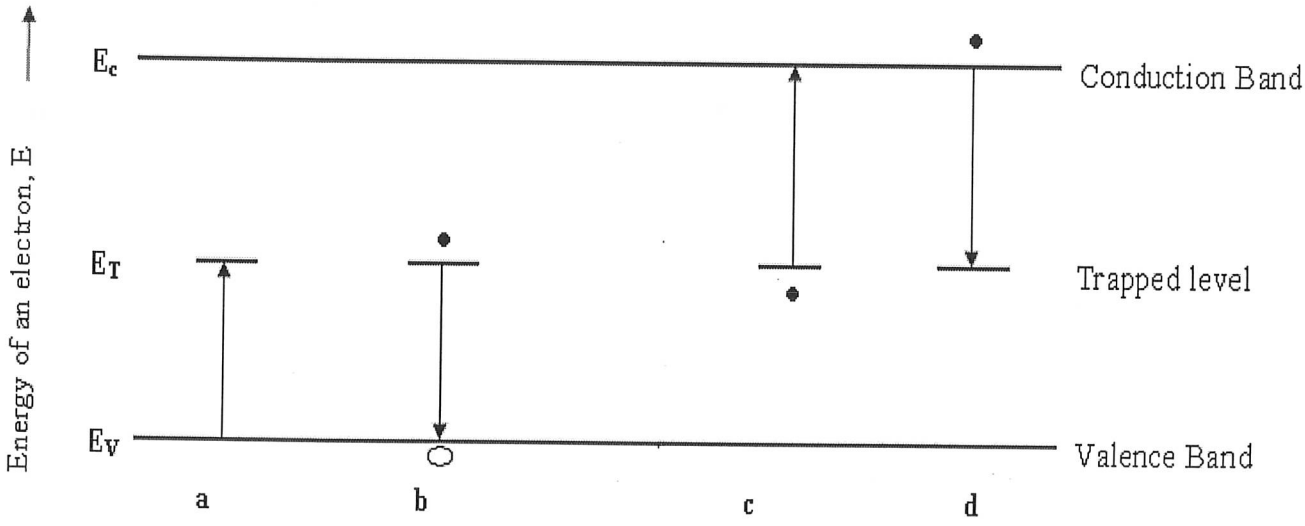

Fig.2.2. *Illustration of transition taking place under non-equilibrium condition.*

The transition taking places under such conditions are illustrated in figure 2.2. It is evident that in addition of four previously mentioned processes (a, b, c, d), another process in which electron leave the valence band and enter the conduction band directly, is taking place.

(a). Electron capture

(b). Hole capture

(c). Electron emission

(d). Hole emission

The expression of Fermi-Dirac distribution function for non-equilibrium conditions can be reformulated by solving equations (2.8-2.10).

$$\frac{dn_T}{dt} = G - (R_d - R_c) \tag{2.8}$$

$$\frac{dp_T}{dt} = G - (R_b - R_a) \tag{2.9}$$

From above equations, under steady non-equilibrium conditions, we get

$$R_d - R_c = R_b - R_a \qquad (2.10)$$

By substituting the values in above equation (2.10), we get the following equation in term of electron and whole concentration.

$$f = \frac{\sigma_n n + \sigma_p n_i e^{\frac{(E_i - E_T)}{k_T}}}{\sigma_n \left[n + n_i e^{\frac{E_T - E_i}{k_T}} \right] + \sigma_p \left[p + n_i e^{\frac{E_i - E_T}{k_T}} \right]} \qquad (2.11)$$

The steady state net rate of recombination $U = R_b - R_a = R_d - R_c$, via the intermediate centers can be obtained by putting the value of 'f' in individual rate process as;

$$U = \frac{\sigma_n n \sigma_p V_{th} N_T (pn - n_i^2)}{\sigma_n \left[n + n_i e^{\frac{E_T - E_i}{k_T}} \right] + \sigma_p \left[p + n_i e^{\frac{E_i - E_T}{k_T}} \right]} \qquad (2.12)$$

When $\sigma_n = \sigma_p = \sigma$, the above expression reduces to;

$$U = \sigma V_{th} N_T \frac{pn - n_i^2}{n + p + 2 n_i \cosh\left(\frac{E_T - E_i}{k_T}\right)} \qquad (2.13)$$

It is clear that the term $pn-n_i^2$ is the 'driving force' **[5]** for the recombination. In fact this is responsible for deviation from equilibrium condition.

The resistance for this process of recombination increase with 'n' and 'p'. it will be smaller when the sum of 'n' and 'p' is at minimum value. The major result of this relationship is the mid-gap levels are dominant recombination centers in semiconductors

and the recombination center is most effective if the two emission probabilities are about the same, i.e. when its energy level is near the middle of energy gap

2.4 Detailed Balance Principle

The principle of detailed balance states as the transition probabilities for the process and its reverse are equal. **[6]**

This principle is used extensively in semiconductor statistics. Blackmore **[5]** Roosbroeck and Shockley **[7]** derived the formula for the carrier lifetime for intrinsic radiative recombination; this approach was extended to extrinsic radiative process by Scalar and Burstein **[8].**

The rate of creation and annihilation of free carrier in the semiconductor at thermal equilibrium is equal and condition is termed as the "Detailed Balance Principle".

Thus according to this principle, the rate of electron emission from the deep level and the rate of electron capture are equal. Similarly, the rate of hole emission and capture are also equal, that is

$$R_b = R_a \tag{2.14}$$

$$R_d = R_c \tag{2.15}$$

Alternatively,

$$e_n N_T f = c_n n N_T (1 - f) \tag{2.16}$$

And

$$e_p N_T (1 - f) = c_p p N_T f \tag{2.17}$$

By the law of mass action

$$np = n_i^2 \tag{2.18}$$

By combining equations (2.16) and (2.17) with (2.18), we obtain

$$e_n e_p = c_n c_p n_i^2 \tag{2.19}$$

This is another way to express the detailed balance relationship.

Using the equation (2.3) and (2.40) with the expression of electron concentration given by equation (2.20-a) in equation (2.15), the electron emission rate is represented as equation (2.20-b),

$$n = N_C \exp - \frac{(E_C - E_F)}{kT} \qquad (2.20\text{-a})$$

$$en = \sigma_n \langle V \rangle_{th} N_C \exp - \frac{(E_c - E_T)}{kT} \qquad (2.20\text{-b})$$

Where 'Nc' and 'E_C' represent the effective density of state in conduction band and the conduction band lower edge energy, respectively.

Similarly the hole emission rate can be obtained by using equation (2.1), (2.2) and hole concentration in equation (2.14), as

$$e_p = \sigma_p \langle V \rangle_{th} N_V \exp - \frac{(E_T - E_V)}{kT} \qquad (2.21)$$

From these equations one can get the thermal activation energy of the trap E_T - E_V *or* E_C - E_T.

2.5 Deep Level Parameters

Various measurements usually performed in characterizing the deep level are listed below:

- Thermal activation energy **(E_a).**
- Photoionization energy.
- Binding energy or photon ionization energy.
- Thermal emission rates **(e_n, e_p).**
- Capture cross-sections **(c_n,c_p / σ_n,σ_p).**
- Photon ionization cross-section **(σ^0_n ,σ^0_p).**
- Concentrations
- Temperature dependence of capture cross-sections.
- Electric field dependence of thermal emission rates.

From all these parameters the most important parameter is thermal activation energy; usually denoted as 'E_a'. Thermal energy of the deep level is defined as the amount of energy needed to eject the trap carrier from the deep level up appropriate energy band. It

provides a measure of energy position in the band gap of semiconductor. It represented as 'E_c - E_T' and 'E_T-E_V ' for electron and hole emission respectively, where 'E_T' and 'E_V' represent the absolute value of energy position of the deep level and upper edge of valence band, respectively. One can further use these parameters to describe a deep level using their dependence on different physical parameters. for example, temperature dependence of capture cross-section (σ) gives us interesting insight into capture of carriers and radiative r non-radiative emission of carriers.

2.6 EL2 Defect in GaAs

EL2 defect is the main defect in melt grown GaAs, This defect is famous because it is present in all bulk materials with relatively large (-10^{16} cm^{-3}) concentrations and in epitaxial layers with low (-$10^{14}cm^{-3}$) concentrations. It compensates the free carriers in undoped or lightly doped materials resulting in their semi-insulating property. This defect has been extensively studied because of its technological importance. **[9]**

For the past few years EL2 became the dominant subject of semiconductor defect physics for reasons reaching far beyond pure scientific interest. To a great extent EL2 defect controls GaAs electrical and optical properties and its presence allows to obtain undoped thermally stable semi insulating (SI) crystals - the key material for integrated circuits technology. However, in spite of much effort put into EL2 studies, there is still no common opinion upon its exact nature, although its connection with antisite arsenic defect is widely accepted. The basic problem is if EL2 is an isolated antisite arsenic defect or a complex involving antisite arsenic.

2.6.1 Characteristics of EL2 in GaAs

A careful discussion of the EL2 center requires us to take a variety of different properties into account. I therefore start with a list of the most important "experimentally established properties of EL2."

- The normal or fundamental state of EL2 (labeled EL2-F in the following) has a deep donor level at mid-gap (E~+0.75 eV).

- EL2-F is an intrinsic deep defect, i.e., impurities do not control its characteristic optical properties.
- EL2- F is a deep double donor: In addition, to the 0/+ level there is a + /2+ level, at $E_v = +0.54$ eV.
- There is no further level of EL2-F in the upper part of band gap.
- The neutral EL2-F exhibits an internal optical transition at $1.0<\hbar\omega<1.3$eV, which contributes to absorption, but only little to conductivity. **[11].**
- Below 140 K, EL2-F can be optically bleached by photons from the internal transition range. The bleaching state of EL2 is labeled as EL2-M.
- The presence of electrons in the conduction band lowers the barrier to 0.1 eV (called electron-induced or Auger-like de-excitation). **[12]**
- By annealing the sample at T =130°C or 850°C, EL2 is regenerated.**[13][14]**

2.6.2 Activation Energy of EL2

The EL2 is located at 0.75 eV, this value is accurate and reliable **[14]**. And give rise to DLTS peak around 360 k and emission rate (e_n) is .017 sec^{-1} (τ=58 sec) **[15].**

$$E_1 = E_T = E_C - 0.75 \text{ eV}$$

2.6.3 Optical Properties of EL2 from Photocapacitance Measurements

As far as ionization of a deep level defect is concerned, the optical properties of a conventional defect are completely characterized by an electron ionization cross-section $\sigma^0_n(h\upsilon)$ and a hole ionization cross section $\sigma^0_p(h\upsilon)$. These quantities describe the relative probability of electron and hole excitation into the conduction and valence bands respectively as a function of photon energy. For the mid-gap level of EL2 these cross-sections have been measured with Deep Level Optical Spectroscopy (DLOS) **[16].**

This is a photocapacitance technique in which the space charge region of a reverse biased Schottky diode is illuminated with monochromatic light to ionize the deep level. This results in a change of the diode capacitance. If this change is recorded as a function of illumination time one obtains a photocapacitance transient. The initial slope of this transient is proportional to σ^0_n or σ^0_p depending on the initial conditions that have

been set (all centers filled with electrons or all centers filled with holes). Scanning the photon energy 'hυ' point by point up to the band edge then provides the complete spectral dependence of the cross-section. In this way σ^0_n (hυ) and σ^0_p (hυ) of the EL2 mid-gap level have been determined **[17]**. They are schematically plotted in figure 2.4. The ratio of $\sigma^0_p/\ \sigma^0_p$ at hυ = 1.17 eV has been adopted from reference **[18]**. Note that the σ^0_n (hυ) curve corresponds to a low temperature measurement, while the σ^0_p(hυ) curve has been measured at room temperature. This difference accounts for the fact that the σ^0_p (hυ) threshold is somewhat below the low temperature mid-gap position, hυ ≈ 0.75 eV. Recent measurements of σ^0_p (hυ) at 80 K **[19]** confirm that its low energy increasing photon energy up to the band edge. Some structure is visible which has been attributed to electron transitions to higher conduction band minima. In contrast the σ^0_p (hυ) curve is peaked near 0.95 eV. In the lower energy region,hυ < 1.1 eV, the value of σ^0_p (hυ) exceeds that of σ^0_n (hυ) while above 1.1 eV the relation is reversed. For hυ ≈1.1 eV the two cross-sections are equal in magnitude.

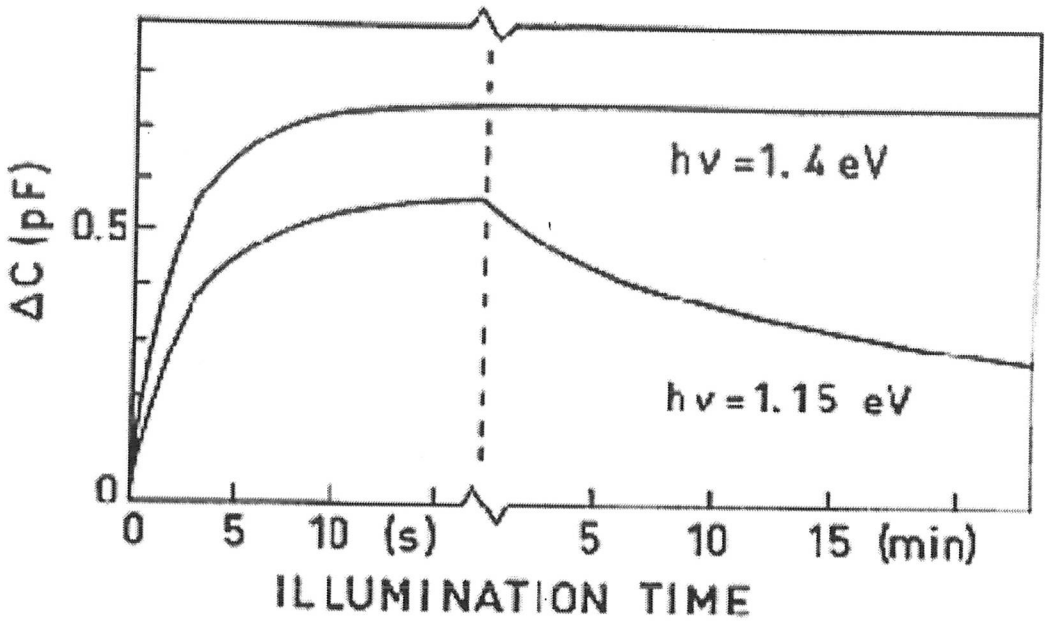

Fig. 2.4: EL2 photocapacitance transients observed on n-GaAs Schottky diodes for two photon energies hυ [21].

Therefore the optical absorption due to the EL2 mid-gap level at this energy is independent of the charge state. Its unusual and peculiar behavior has also discovered by photocapacitance measurements **[17] [20] [21].**

These studies revealed that a third optical cross-section, σ_*° is required to fully describe the photoresponse of the mid-gap level. The unusual behavior is apparent only at temperatures below 120K and only in a narrow range of photon energies, 1.0 eV < hυ <1.4 eV. It manifests in the following way. Assume that photocapacitance experiment is performed under the above conditions and with all mid-gap levels filled with electrons before illumination. In this case the capacitance transient first increases (due to electron emission), see the hυ =1.15 eV transient in figure 2.4. This anomalous phenomenon is called the persistent photocapacitance quenching (PPCQ) effect. In contrast, the normal photocapacitance behavior is given by the monotonic hυ = 1.4 eV transient in figure 2.4.

2.7 HM1 Defect in p-type GaAs

The study of inadvertent (intrinsic) deep levels in p-GaAs has attracted less attention as compared to that of intentionally introduced deep levels in this material. Although some work has been performed on the dominant inadvertent deep level observed around ~ Ev+0.55 eV in nearly all p-type GaAs materials grown by different techniques its identification remains inconclusive. Most of the researchers have attributed this level to Fe. In Bridgman-grown GaAs, Lagowski et al. **[10]** identified this inadvertent deep level, labeled by them as HM1, with the doubly charged state of the well-known native defect EL2. Both these researchers have made tentative identification of this level without providing any concrete evidence.

2.8 References

1. W. Kohn and I. M. Luttinger, Phys. Rev. 98,915 (1955).
2. Hall, R.N., Electron-hole recombination in Germanium, Phys. Rev. 87 (1952), pp. 387.
3. Shockley, W., Read, W.T., Statistics of the Recombinations of Holes and Electrons, Phys. Rev. 87 (1952), pp. 835–842.
4. Thierry Goudon, Vera Miljanovi´c, Christian Schmeiser January 17, 2006.
5. J.S Blackmore, Semiconductor Statistics, Pergamon Press, Oxford, N.Y (1981).
6. Charles Kittle, Elementary statistical Physics, Wiley, New York (1958).
7. Von Roosbroeck and W. Shockley, Phys. Rev. 94, 1558, (1954).
8. N.Sclar and E. Burstein, Phys. Rev. 98, 1757, (1955).
9. M. Kaminska Institute of Experimental Physics, Warsaw University, Hoza 69, 00-68 1 Warsaw, Poland, June 9, 1987.
10. M. Kaminska, M. Skowronski, and W. Kuszko, Phys. Rev. Lett. 55, 2204 (1985).
11. M. A. Zaidi, H. Maaref and J. C. Bourgion, Appl. Phys. Lett, 60,2183 (1988).
12. H. J. von Bardeleben, D. Stievenard, D. Deresmes, A. Huber, and J. C. Bourgoin, Phys. Rev. B 34, 7192 (1986).
13. J. Lagowski, H. C. Gatos, C. H. Kang, M. Skowronski, K. Y. Ko, and D. G. Lin, Appl. Phys. Lett. 49, 892 (1986).
14. D.C. Look*, Z.-Q. Fang Semiconductor Research Center, Wright State University, Dayton, OH 45435, USA, 25 March 1999.
15. CHANTRE, A., VINCENT, G. and BOIS, D., Phys. Rev. B 23 (1981) 5335.
16. B. Dischler and U. Kaufmann Fraunhofer-Institut für Angewandte Festkörperphysik, Eckerstr. 4, D-7800 Freiburg, F.R.G. (1987)
17. VINCENT, G., BOIS, D. and CHANTRE, A., J. Appl. Phys. 53 (1982) 3643.
18. MARTIN, G., Semi-insulating III-V Materials, Ed. G. Rees (Shiva Ltd. Orpington) 1980, p. 13.
19. MORANTE, J. R., SAMITIER, J., PEREZ, A., ALTELARREA, H. and GOURRIER, S., J. Appl. Phys. 60 (1986) 1661.
20. BOIS, D. and VINCENT, G., J. Physique 38 (1977) L 351.
21. VINCENT, G. and BOIS, D., Solid State Commun. 27 (1978) 431.

Chapter 3

Photocapacitance Technique

3.1 Introduction

Defects in semiconductors are used to control the concentration and lifetime of charge carriers which in turn determine the properties of the materials. The identification and characterization of the defects is therefore of utmost importance.

The basic characterization of defects in semiconductors involves the knowledge of their geometrical structure, electronic configuration, electrical activity related to band-gap states and dynamical properties which characterize mutual defect interactions and interactions with the lattice. A number of experimental techniques have been have been used for the study of deep levels in semiconductors. Here we discuss the brief introduction of some important techniques.

The various experimental techniques have been employed to investigate the deep level in semiconductor materials. One class of technique, the junction space-charge technique is very commonly used. In thermal stimulated current (TSC) and the thermal stimulated capacitance (TSCAP), measurement of shift of the peak is taken as function of rate of heating. The stimulated and carrier emission from the deep levels is reverse in carrier in bias junction. In isothermal single shot dark transient technique, the junction is maintained at constant temperature during the measurement. The full current or capacitance transients recorded during the carrier emission from the deep level after the carrier is switched to reverse bias from the zero or the forward bias.

Similarly Deep Level Transient Spectroscopy (DLTS) is an experimental tool for studying electrically active defects (known as charge carrier traps) in semiconductors. DLTS establishes fundamental defect parameters and measure their concentration in the material. Some of the parameters are considered as defect "finger prints" used for their identifications and analysis.

DLTS investigates defects present in a space charge (depletion) region of a simple electronic device. The most commonly used are Schottky diodes or p-n junctions. In the measurement process the steady-state diode reverse polarization voltage is disturbed by a voltage

pulse. This voltage pulse reduces the electric field in the space charge region and allows free carriers from the semiconductor bulk to penetrate this region and recharge the defects causing their non-equilibrium charge state. After the pulse, when the voltage returns to its steady-state value, the defects start to emit trapped carriers due to the thermal emission process. The technique observes the device space charge region capacitance where the defect charge state recovery causes the capacitance transient. The voltage pulses followed by the defect charge state recovery are cycled allowing an application of different signal processing methods for defect recharging process analysis.

The DLTS technique has a higher sensitivity than almost any other semiconductor diagnostic technique. For example, in silicon it can detect impurities and defects at a concentration of one part in 1012 of the material host atoms. This feature together with a technical simplicity of its design made it very popular in research labs and semiconductor material production factories.

The DLTS technique was pioneered by D. V. Lang (David Vern Lang of Bell Laboratories) in 1974. [1] US Patent was awarded to Lang in 1975. Photocapacitanc is very sensitive technique for detecting the deep traps whether they are radiative or non-radiative and it allows a determination of exactly the properties needed to specify the role of trap in electron-hole recombination. The radiaive recombination process have a negligible rates in indirect material such as 'Si' and 'Ge', but these processes are very important in direct band gap materials, such as 'GaAs', specialy when the carrier concentration is very high [2].

This is an optical single-shot measurement technique quite analogous to the dark capacitance transient technique, with the only difference being that the excitation processes are optically induced rather than thermally. As already mentioned, these experiments are usually performed at very low temperatures (<80K) to avoid any contributions to the capacitance transients from thermal excitation processes and also to avoid phonon-broadening effects. Suppose that the deep level to be studied is situated in the upper half of the band gap. By short-circuiting the diode the deep levels in the transition region are filled as previously described. These filled traps may now be emptied by light provided the photon energy exceeds the binding energy of the electrons. Furthermore, if the photon energy is limited to half of the energy band gap, only electron transitions to the conduction band may occur.

Photocapacitance can be extended to provide the minority carrier capture rates ($c_n = \sigma_n \upsilon_n n$). this is achieved by suitably forward biasing the junction, thereby injecting free carrier into neutral materials, the subsequently reverse biasing the device allow a capacitive determination of the resulting change in the trapped charges [3].

In Photocapacitance technique we measure capacitance change by illuminating the sample with light. The variation of junction capacitance follows the emission of trap carriers. The capacitance varies as an exponent function of time until the traps are emptied or filled, where the constant value of capacitance C (∞) is attained. The difference between the initial and final value of capacitance, under these conditions is measure of the total concentration of deep traps. The change in capacitance depends upon the temperature and depth of deep center [4]. At any time after the light was switched on, the capacitance of the junction is given by

$$C(t) = C(\infty)\left[1 - \exp\left(\frac{-t}{\tau}\right)\right] \qquad \text{(For majority carriers)} \qquad (3.1)$$

$$C(t) = C(\infty)\exp\left(\frac{-t}{\tau}\right) \qquad \text{(For minority carrier)} \qquad (3.2)$$

Where τ is the time constant of the capacitance change of the transient. The capacitance is expected to increase for the majority carriers and decrease for the minority carriers traps. The total change in capacitance $\Delta C = C(\infty) - C(t)$ is obtained and $\ln[\Delta C]$ is plotted as a function of time. The straight line thus obtained which provides the information about the emission rates of electrons and traps.

3.2 Kinetic process.

The electron-hole pair recombination can take place mainly by two ways, either by direct recombination of conduction band electron with valence band hole or electron-hole recombines through deep level. For deep level having energy ET, four basic emission and captures processes takes place. The rate of these processes are given by

$R_a = c_n\, np_T$

$R_b = e_n\, n_T$

$R_c = c_p p n_T$

$R_d = e_p p_T$

Where

e_n, e_p(1/sec) are proportionality constant defined as electron and hole emission rates, $c_n = \sigma_n \upsilon_{th}$ and $c_p = \sigma_p \upsilon_{th}$ are the electron and hole capture coefficients (cm^3/sec). Capture rates of electron and hole depend upon the cross-section of trap (σ_n, σ_p) and on average thermal velocity (v_{th}) of conduction/valance band electron/hole. 'n' and 'p' are the densities of electrons and holes in conduction and valance band, 'n_T', 'p_T' are concentration of level filled and empitied of electron and electron or occupied by hole. If G-R center is donar, n_T is negatively charged and p_T is positively charged. For an acceptor G-R center. nT is negatively charged and p_T is neutral. The total density is given by

$$N_T = n_T + p_T \tag{3.3}$$

The electron density in the conduction band diminished by electron capture and increase by electron emission process. The rate of change of carrier concentration in the bands due to these thermal and optical processes at defect centers is given by

$$-\left(\frac{dn}{dt}\right)_T = (a^t) - (b^t) + (a^\circ) - (b^\circ)$$

$$= c^t{}_n np_T - e^t{}_n n_T + c^\circ{}_n n_T - e^\circ{}_n n_T$$

$$\left(\frac{dn_T}{dt}\right) = e_n n_T - c_n np_T \tag{3.4}$$

$$-\left(\frac{dp}{dt}\right) = c^t{}_p pnt - e^t{}_p p_T + c^\circ{}_p pn_T - e^\circ{}_p p_T$$

$$\left(\frac{dp_T}{dt}\right) = e_p p_T - c_p pn_T \tag{3.5}$$

The combined optical and thermal rate constants are denoted by cn, cp, en and ep.

Where

$$c_n = ct_n + c°_n$$

And

$$e_n = e^t_n + e°_n$$

3.3 Electron/hole occupancy of deep levels

3.3.1 Electron occupancy of deep levels

When an electron/hole is captured or emitted, the center occupancy changes of an energy level changes and the rate of change of an occupancy level is given by

$$\frac{dn}{dt} = \frac{dp(t)}{dt} - \frac{dn(t)}{dt}$$

$$= (r_d - r_c) - (r_b - r_a)$$

$$\frac{dn_T}{dt} = (e_p p_T - c_n p n_T) - (e_n n_T - c_n n p_T) \quad (3.6)$$

Where

$$e_n = e_n^t + e_n^0, e_p = e_p^t + e_p^0$$

$$\frac{dn(T)}{dt} = (e_p^t + e_p^0 + c_n n)\, p_T - (e_n^t + e_n^0 + c_p p)\, n_T$$

$$\frac{dn(T)}{dt} = (e_p^t + e_p^0 + c_n n)(N_{TT} - n_T) - (e_n^t + e_n^0 + c_p p)\, n_T \quad (3.7)$$

Under steady state as t$\longrightarrow\infty$, the electron occupancy is given by

$$\frac{n_T}{N_{TT}} = \frac{e_p^t + e_p^0 + c_n n}{(e_p^t + e_p^0 + c_p p + e_n^t + e_n^0 + c_n n)} \quad (3.8)$$

Equation 3.8 gives the density of filled traps with electrons under steady state condition, when both electron and holes emission rates are significant.

At low temperature (below the freeze out region), the thermal emission rate can be neglected. $(e_p^t = e_n^t = 0)$,

Therefore 3.7 can be written as

$$\frac{dn(T)}{dt} = (e_p^0 + c_n n)(N_{TT} - n_T) - (e_n^0 + c_p p)n_T \tag{3.9}$$

Under illumination the charge in electron occupancy is given by

$$\Delta n_T = \frac{e_p^0}{e_n^0 + e_n^0} N_{TT} \tag{3.10}$$

Rearranging and integrating eq 3.9 from t=0 to any time "t" with occupancy of levels filled with electrons $n_T(0)$ and $n_T(t)$ respectively.

$$\int_{n_T(0)}^{n_T(t)} \frac{dn_T(t)}{\left[N_{TT}\left(\frac{e_p^0 + c_n n}{(e_p^0 + c_p p + e_n^0 + c_n n)}\right) - n_T(t)\right]}$$

$$= [(e_p^0 + c_p p + e_n^0 + c_n n)] \int_0^t dt - ln\left[N_{TT}\left(\frac{e_p^0 + c_n n}{(e_p^0 + c_p p + e_n^0 + c_n n)}\right) - n_T(t)\right]$$

$$+ ln[N_{TT}\left(\frac{e_p^0 + c_n n}{(e_p^0 + c_p p + e_n^0 + c_n n)}\right) - n_T(0)]$$

$$= [e_p^0 + c_p p + e_n^0 + c_n n]t$$

Taking exponential and rearranging the terms

$$n_T(t) = N_{TT}\left(\frac{e_p^0 + c_n n}{(e_p^0 + c_p p + e_n^0 + c_n n)}\right) + [-N_{TT}\left(\frac{e_p^0 + c_n n}{(e_p^0 + c_p p + e_n^0 + c_n n)}\right) + n_T(0)]e^{-(e_p^0 + c_p p + e_n^0 + c_n n)t} \tag{3.11}$$

$$n_T(t) = n_T(0)]e^{-t/r} + N_{TT}\left(\frac{e_p^0 + c_n n}{(e_p^0 + c_p p + e_n^0 + c_n n)}\right)[1 - e^{-\frac{t}{r}}] \tag{3.12}$$

Eq.3.11 shows that when light of particular wavelength is shone, the time constant of the transient change in electron occupancy of a deep level is given by

$$\tau = \frac{1}{(e_p^0 + c_p p + e_n^0 + c_n n)} \tag{3.13}$$

Where $n_T(0)$ is the density of G-R centers occupied by electrons at t=0

$$n_T(0) = N_{TT}$$

Consider the trap in the upper half of the bandgap with $e_n \gg e_p$ allowing $e_p = 0$ in equation 3.12 during the initial emission period, the time dependence of n_T simplifies to

$$n_T(t) = n_T(0)]e^{-t/r} \approx N_{TT}e^{-t/r} \tag{3.15}$$

With $\tau_r = \frac{1}{e_n}$ following the electron emission traps, holes remain and are subsequently emitted by electron emission. Some traps are in n_T and some traps are in p_T state. When the diode is pulsed from reverse bias to zero bias, electrons rush into be captured by traps in the p_T state. The time dependence of during the capture period is

$$n_T(t) = N_{TT} - [N_T - n_{TT}(0)]e^{-t/r}$$

Where $\tau_r = \frac{1}{c_n\, n}$ and is initial steady state density given by

$$n_T = \frac{e_p}{e_p + e_n} N_{TT} \tag{3.16}$$

3.3.2 Hole occupancy of deep levels

The rate of change of hole occupancy is given by

$$\frac{dp_T}{dt} = \frac{d(t)}{dt} - \frac{dp(t)}{dt}$$

$$= (r_b - r_a) - (r_d - r_c)$$

$$\frac{dp_T}{dt} = (e_n n_T - c_n n p_T) - (e_p p_T - c_n p n_T) \tag{3.17}$$

$$\frac{dp_T}{dt} = (e_n^t + e_n^0 + c_p p)(N_{TT} - p_T) - (e_p^t + e_p^0 + c_n n)\, p_T \tag{3.18}$$

Under steady state as t→∞, the electron occupancy is given by

$$\frac{p_T}{N_{TT}} = \frac{e_n^t + e_n^0 + c_p p}{(e_p^t + e_p^0 + c_n n + e_n^t + e_n^0 + c_p p)} \tag{3.19}$$

Eq 3.19 gives the density of filled trap with holes under steady state condition, when both electrons and holes emission rates are significant.

At low temperature (below the freeze out region), the thermal emission rate can be neglected therefore ($e_p^t = e_n^t = 0$) eq 3.18 can be written as

$$\frac{dp_T}{dt} = (e_n^0 + c_p p)(N_{TT} - n_T) - (e_p^0 + c_n n)\, n_T \tag{3.20}$$

Rearranging and integrating the eq 3.20 from t=0 to any time "t" with occupancy levels filled with electrons $p_T(0)$ and $p_T(t)$respectively.

$$\int_{p_T(0)}^{p_T(t)} \frac{dp_T(t)}{\left[N_{TT}\left(\frac{e_n^0 + c_p p}{(e_p^0 + c_p p + e_n^0 + c_n n)}\right) - p_T(t)\right]}$$

$$= [(e_p^0 + c_p p + e_n^0 + c_n n)] \int_0^t dt - ln\left[N_{TT}\left(\frac{e_n^0 + c_p p}{(e_p^0 + c_p p + e_n^0 + c_n n)}\right) - p_T(t)\right]$$

$$+ ln[N_{TT}\left(\frac{e_n^0 + c_p p}{(e_p^0 + c_p p + e_n^0 + c_n n)}\right) - p_T(0)]$$

$$= [e_p^0 + c_p p + e_n^0 + c_n n]t$$

Taking exponential and rearranging terms

$$p_T(t) = N_{TT}\left(\frac{e_n^0 + c_p p}{(e_p^0 + c_p p + e_n^0 + c_n n)}\right) + [-N_{TT}\left(\frac{e_n^0 + c_p p}{(e_p^0 + c_p p + e_n^0 + c_n n)}\right) + p_T(0)]e^{-(e_p^0 + c_p p + e_n^0 + c_n n)t} \tag{3.21}$$

$$p_T(t) = p_T(0)e^{-\frac{t}{\tau}} + N_{TT}\left(\frac{e_n^0 + c_p p}{(e_p^0 + c_p p + e_n^0 + c_n n)}\right)[1 - e^{-\frac{t}{\tau}}] \tag{3.22}$$

In eq 3.11 shows that when light of particular wavelength is shone, the time constant of the transient change in electron occupancy of a deep level is given by

$$\tau = \frac{1}{(e_p^0 + c_p p + e_n^0 + c_n n)} \tag{3.23}$$

Where $n_T(0)$ is the density of G-R centers occupied by electrons at t=0

$$p_T(0) = N_{TT}$$

Consider the trap in the lower half of bandgap with $e_p \gg e_n$ allowing $e_n = 0$ in eq 3.22. During the initial emission period, the time dependence of p_T simplifies to

$$p_T(t) = p_T(0)e^{-\frac{t}{\tau}} \approx N_{TT}e^{-\frac{t}{\tau}} \tag{3.24}$$

$$p_T(t) = N_{TT} - [N_{TT} - n_{pT}(0)]e^{-\frac{t}{\tau}} \tag{3.25}$$

Where

$$\tau_c = \frac{1}{c_p p}$$

3.4 P-n junction

A p-n junction works as a charge storing device in which the total stored charge lies in the space charge region, resulting from the ionized acceptor donor impurities. The capacitance C for a one-sided step junction, under reverse bias is given by

$$C = \sqrt{\frac{A^2 q \varepsilon_0 K_s N_I}{2(V_R + V_b)}} \tag{3.26}$$

Where A id the area of the junction, V_b is the built potential, V_R is the reverse bias, ε_0 is permittivity of free charges, N_I is the impurity density in low doped side space charge region. The ionized shallow –level donors (dopant atom) in the space charge region are positively charged and $N_I = N_D^+ + n_T^-$ for deep level acceptor impurity that are negatively charged when occupied by electrons. When occupied by hole deep level acceptor are neutral and $N_I = N_D^+$ for deep levels occupied the hole $N_I = N_D^+ + p_T^+$ for shallow level donors and deep levels occupied by electrons $N_I = N_D^+$. For p^+n junction the contribution of the deep levels to N_I depends upon the acceptor or donor nature of level.

$$N_I = N_D - n_T \{for\ acceptor\ like\ impurity\}$$

$$N_I = N_D \{for\ donor\ like\ impurity\}$$

Where N_D is the shallow donor concentration.

3.4.1 Junction capacitance change due to electron occupancy of deep level

In capacitance measurements, it is the time varying width W that is detected as change in capacitance. The capacitance of one sided step junction is given by

$$C = \sqrt{\frac{A^2 q \varepsilon_0 K_s N_I}{2(V_R + V_b)}} \tag{3.26A}$$

$$C = \sqrt{\frac{A^2 q \varepsilon_0 K_s (N_D - n_T)}{2(V_R + V_b)}}$$

$$C = \sqrt{\frac{A^2 q \varepsilon_0 K_s (1 - \frac{n_T}{N_D})}{2(V_R + V_b)}}$$

$$C = A \sqrt{\frac{q \varepsilon_0 K_s}{2(V_R + V_b)}} \sqrt{(1 - \frac{n_T}{N_D})} \tag{3.27}$$

In transient capacitance measurement, the deep levels impurities from only a small fraction of the space charge region impurity density, i.e., $N_T \ll N_D$ using binomial extension for eq 3.27 gives

$$C = C_0[1 - \frac{n_T}{N_D}] \tag{3.28}$$

Where C_0 is the capacitance of the device with no deep level impurity at reverse bias.

Emission of majority careers

The junction device is initially zero biased, allowing impurities to capture majority carriers. The capacitance is the zero biased value C(V=0). Following a reverse bias pulse, majority carriers are emitted as a function of time. Now by substituting eq 3.18 into eq 3.28 the result is

$$C = C_0[1 - \frac{n_T(0)}{2N_D} e^{-\frac{t}{\tau_e}}] \tag{3.29}$$

When electrons are emitted from the traps and holes remain on the trap. For deep donor impurities are initially neutral, when occupied by electrons, and space charge region impurity density at t=0 is N_D. As electrons are emitted, the traps become positively charged, and the final charge is $q[N_D + p(\infty)]$. the capacitance increases with time regardless of whether the deep levels impurities are donor or acceptor.

Then for change in capacitance from time t_1 to time t_2 is given by equation 3.26A

$$\Delta C = C(t_2) - C(t_1)$$

$$\Delta C = [\frac{n_T(t_2) - n_T(t_1)}{2}] \sqrt{\frac{A^2 q \varepsilon_0 K_s}{2N_D(V_R + V_b)}} \tag{3.30}$$

Eq 3.30 shows that the change in capacitance is directly proportional to the change in electron occupancy of deep level.

Emission of minority carriers

When the diode is forward bias, holes are injected into n-side and capture dominates over emission. The steady state G-R center occupancy is from eq 5.8 is

$$n_T = \frac{c_n n}{c_n n + c_p p} N_{TT}$$

Which depends on the capture coefficient and both carrier densities. Now consider $c_p \gg c_n$ and $p \approx n$ then most traps are occupied by holes, and for deep level acceptor impurity the centers are neutral. When junction is pulsed to reverse bias, holes are emitted from traps, the charge changes from neutral to negative, and $N_I = N_D - n_T$ for $t \to \infty$. the total ionized space charge region density decreases, the space charge width increases, and the capacitance decreases with time.

Traps in the upper half of the bandgap are detected with majority carrier pulse, those in the lower half of the bandgap are detected by minority carrier pulse for n-type substrate.

Minority carriers can be injected by shining light on sample. Initially the device is zero biased and all the traps are filled with electrons at low temperature. The sample is held at sufficiently low temperature so that the thermal emission rate is negligible but optical emission rate takes place. Light is shone on sample. For $h\nu\rangle(E_c - E_T)$, there is no band-gap optical absorption. For $h\nu\rangle(E_c - E_T)$, photons are excited from the traps into the conduction band. These optical experiments are used to determine the optical properties of the traps, such as the optical cross section and multiplicity of charge states by varying the energy of incident light. For center with donor levels, one increases the light energy to excite electrons from the upper level into the conduction, detected by capacitance change. Increasing the energy further leaves the capacitance unchanged, provided all been excited out of that level, until the energy is sufficient to excite electrons from the second level into the conduction band.

A second capacitance rise is seen. For hole the change in capacitance is given by

$$\text{——}\quad\text{——} \tag{3.31}$$

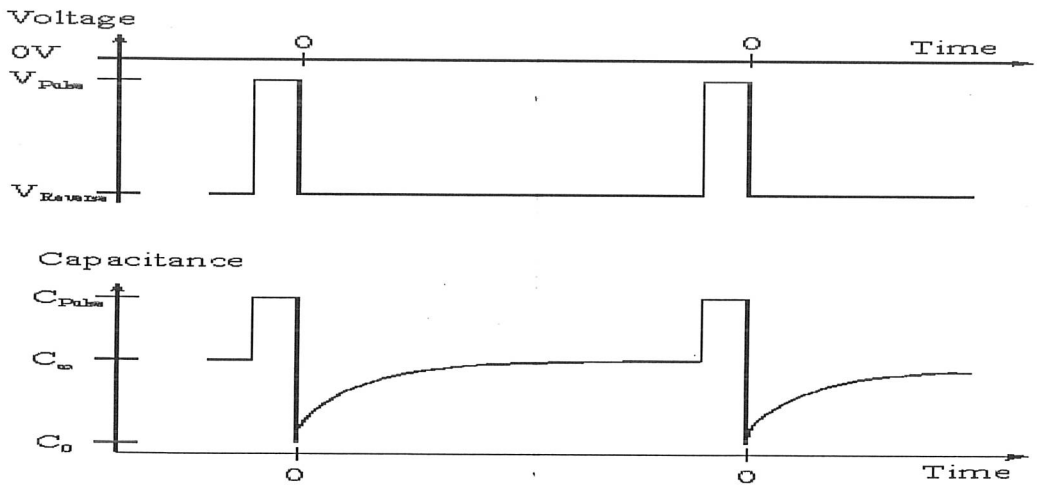

Fig.3.1 Capacitance transient for majority carrier emission

3.5 Optical emission rate

The experimentally accessible emission rates or capture constants. For instance, the optical emission ratee^0 is related to the photoionization cross section σ^o by the relation

$$e^0 = \sigma^o \Phi \tag{3.32}$$

Where Φ is the optical flux of photons.

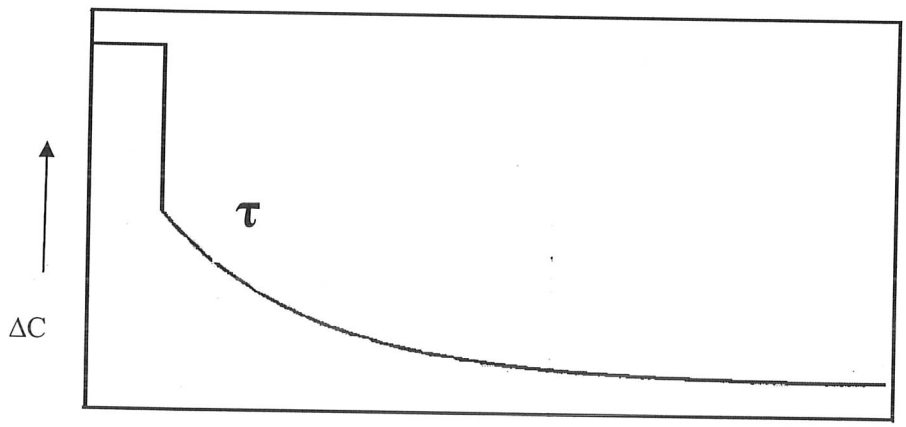

Fig.3.2: Capacitance for minority carrier emission.

3.6 Electron/hole photoionization cross section

3.6.1 Electron photoionization cross section from initially filled with electrons condition to final steady state value

The occupancy of the levels filled with the electrons at any time t is given by eq 3.11 for the initial condition that all the levels were filled with electrons at time t=0

$$n_T(t_1) = n_T(0) = N_{TT} \tag{3.32A}$$

For any time t

$$n_T(t_2) = n_T(t) = N_{TT}\left(\frac{e_p^0}{e_p^0+e_n^0}\right) + [N_{TT}\left(\frac{e_p^0}{e_p^0+e_n^0}\right)]e^{-(e_p^0+e_n^0)t} \tag{3.33}$$

Then for $t = \infty$ the second term of eq 3.33 vanishes, and eq becomes

$$n_T(t_2) = n_T(\infty) = N_{TT}\left(\frac{e_p^0}{e_p^0+e_n^0}\right) \tag{3.34}$$

So e_p^0 can be obtained under the above described conditions by putting eq 3.32A & eq 3.34 in eq 3.30.

$$\Delta C = \left[\frac{N_{TT} - N_{TT\frac{e_p^0}{e_p^0+e_n^0}}}{2}\right]\sqrt{\frac{A^2 q\varepsilon_0 K_s}{2N_D(V_R+V_b)}}$$

$$\Delta C = \left[\frac{N_{TT\frac{e_p^0}{e_p^0+e_n^0}}}{2}\right]\sqrt{\frac{A^2 q\varepsilon_0 K_s}{2N_D(V_R+V_b)}}$$

$$\Delta C = \frac{[e_n^0\, \Phi\, \tau Z_1]}{\Phi}$$

$$Z_1 = constant\ t = \frac{N_{TT}}{2\left[\sqrt{\frac{A^2 q\varepsilon_0 K_s}{2N_D(V_R+V_b)}}\right]}$$

Where $\tau = \frac{1}{e_p^0+e_n^0}$, Φ is the photon flux.

The electron photoionization is given by eq 3.32

$$\sigma^o = \frac{e^0}{\Phi}$$

$$\sigma_n^0 = \frac{\Delta C}{\Phi\, \tau Z_1} \tag{3.35}$$

Where τ can be obtained experimentally from the time constant of the capacitance transient, the magnitude of the full transient giving ΔC . Thus knowing N_{TT} (from DLTS measurement) and N_D from C-V data, σ at a particular hϑ of the incident radiation and known photon flux can be measured.

3.6.2 Hole photoionization cross section from initially filled with electron condition to final steady state value

Since

$$\tau = \frac{1}{(\sigma_p^0 + \sigma_n^0)\Phi}$$

Therefore eq 3.35 can be written as

$$\sigma_n^0 = \frac{\Delta C[(\sigma_p^0 + \sigma_n^0)]\Phi}{\Phi Z_1}$$

$$\sigma_p^0 = \sigma_n^0 [\frac{Z_1}{\Delta C} - 1] \quad (3.36)$$

3.6.3 Hole photoionization cross section from initially filled with hole condition to final steady state value

The occupancy of the levels filled holes at any time t is given by eq 3.21 for initial condition that all the levels are filled holes at t=0

$$p_T(t_1) = p_T(0) = N_{TT} \quad (3.36A)$$

And at time t is

$$p_T(t_1) = p_T(0) = N_{TT}\left(\frac{e_n^0}{e_p^0+e_n^0}\right) + [N_{TT}\left(\frac{e_n^0}{e_p^0+e_n^0}\right)]e^{-(e_p^0+e_n^0)t} \quad (3.37)$$

And for time $t = \infty$ eq 3.37 can be written as

$$p_T(t_2) = p_T(\infty) = N_{TT}\left(\frac{e_n^0}{e_p^0+e_n^0}\right) \quad (3.38)$$

Now by putting 3.37A & 3.28min eq 3.30, the result is

$$\sigma_p^0 = \frac{\Delta C}{\Phi \tau Z_1} \quad (3.39)$$

3.6.4. Electron photoionization cross section from initially filled with hole condition to final steady state value

From eq 3.39

$$\sigma_p^0 = \frac{\Delta C}{\Phi \tau Z_1}$$

$$\sigma_n^0 = \frac{\Delta C(\sigma_p^0 + \sigma_n^0)\Phi}{\Phi Z_1}$$

$$\sigma_n^0 = \sigma_p^0[\frac{Z_1}{\Delta C} - 1] \quad (3.40)$$

3.6 Electron/Hole Photoionization Cross-section from initial slope method.

From the capacitance full transient (transient taken by shining a particular energy light from initially filled conduction to steady state value) gives information about the total capacitance change ΔC and the time constant of the transient, with the information about total capacitance change ΔC and the time constant of the transient. With this information electron/hole photoionization cross-section can be obtained. If instead of photocapacitance full transient which take part too long time, the transient which can take up to that part on which straight line can be fitted, the job of calculation become very easy. It is known that for particular photon energy light, this initial slope of transient is proportional to time constant τ obtained from the full transient for the same photon energy.

Initial slope (m) α τ

$$\tau = \frac{m}{constant}$$

$$\tau = \frac{1}{[\sigma^\circ_n + \sigma^\circ_p]\Phi}$$

$$(\sigma^\circ_n + \sigma^\circ_p) = \frac{1}{\tau\Phi} \quad (3.41)$$

The initial slope of quenching

$$\frac{1}{\tau} = \frac{1}{\Delta C_0}\frac{d\Delta C}{dt}$$

The spectral distribution can be obtained by plotting the ($\tau\Phi$)-1 versus hυ

3.7 Measurements of the deep levels concentration N_{TT}

The concentration deep centers can be measured by using the photocapacitance technique. These measurements are performed below the freeze out temperature ($e^t_n = e^t_p = 0$), by reverse biasing a p^+-n junction [nt(0)=N_{TT}] and illuminating with photons of energy smaller than the band-gap ($e°_p = 0$). The total change in capacitance is given by

$$\Delta C = N_{TT}\frac{1}{2}\sqrt{\frac{A^2 q\varepsilon o K_s}{2N_D(V_R+V_b)}} \qquad (3.42)$$

3.9 References

1. D.V. Lang, "Deep-level transient spectroscopy: A new method to characterize traps in semiconductors", J. Appl. Phys., vol. 45 (1974) 3023.
2. C. T. Sah, L. Forbes. L. L. Rosier and A. F. Tasch, JR. Solid State electronics, 13, 759(1970).
3. C. H. Henry, H. Kukimotto, G. L. Miller and F. R. Merritt, Phy. Rev B, 7, 2499(1973). Richard Willium. J. Appl. Phys. 37, 3411 (1966).

Chapter 4

Experimental Details

4.1 Current-Voltage (I-V) Measurements

The I-V characterization is one of the important measurements because the reverse leakage current of the junction diode has to be low for the capacitance measurements. The I-V measurements were performed with an Advantest digital electrometer. The electrometer has a built-in DC power supply, which is capable of supplying up to 30 volts. The current can be measured in the range of 1pA to 2.2mA. The Block diagram of the set-up for I-V measurements is shown in Fig. 4.1.

4.2 Capacitance-Voltage (C-V) Measurements

To characterize the deep level contents of a diode, it is necessary to have knowledge about its shallow level density, shallow level doping profiles as well as the built-in voltage and the type of junction. C-V measurements provide such information. Therefore, C-V measurements are necessary when one is using any capacitance-based technique including photocapacitance technique. A C-V plot gives us the following information

1. Type of the junction i.e. step or linearly graded
2. Built-in voltage V_B of p-n junction
3. Concentration of shallow dopants N_D, N_A

N_D can be calculated from the (C-V) plot by the following calculations.

$$\text{Slope if C-V plot} = \frac{d\left(\frac{1}{C^2}\right)}{dV_R} = \frac{2}{\varepsilon_S q A^2 N_D}$$

Therefore

$$N_D = \frac{2}{\varepsilon_S} qA^2 \left[\frac{d\left(\frac{1}{C^2}\right)}{dV_R} \right]$$

The C-V measurements are performed by using a Boonton 72-B capacitance meter with Phillips PE-1514 DC power supply. The output analog signal from the capacitance meter along with the variation in voltage was recorded.

4.3 Deep Level Transient Spectroscopy (DLTS) Measurements

The DLTS measurements were carried out using a DLS-81 deep level spectrometer. This DLS-81 system consists of a fast response, 1MHz capacitance/conductance meter with built-in local-in amplifier and double pulse generator. The prominent feature of this system is its high sensitivity. The block diagram of the set-up is given in Fig.4.2

The DLTS scan of a sample reveals the presence of deep levels in the sample. DLTS measurements are also very useful in measuring the deep level concentration.

4.4 Experimental set-up for Photocapacitance measurement.

The photocapacitance technique, in general, consists of illumination of p-n junction at a stabilized temperature, low enough for the thermal transitions to be neglected. So that only optical transition could be studied. The block diagram of the experimental set-up is shown in Fig. 4.3.

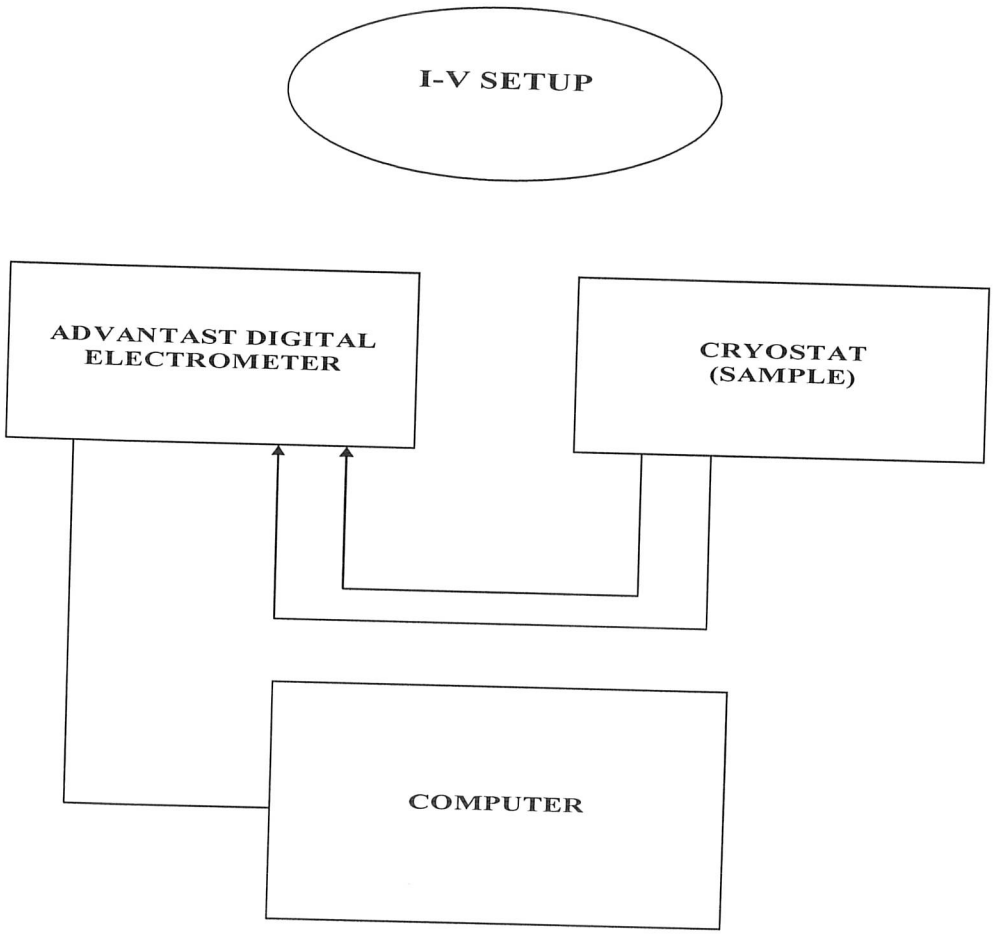

Fig.4.1 Block Diagram Of I-V measurements.

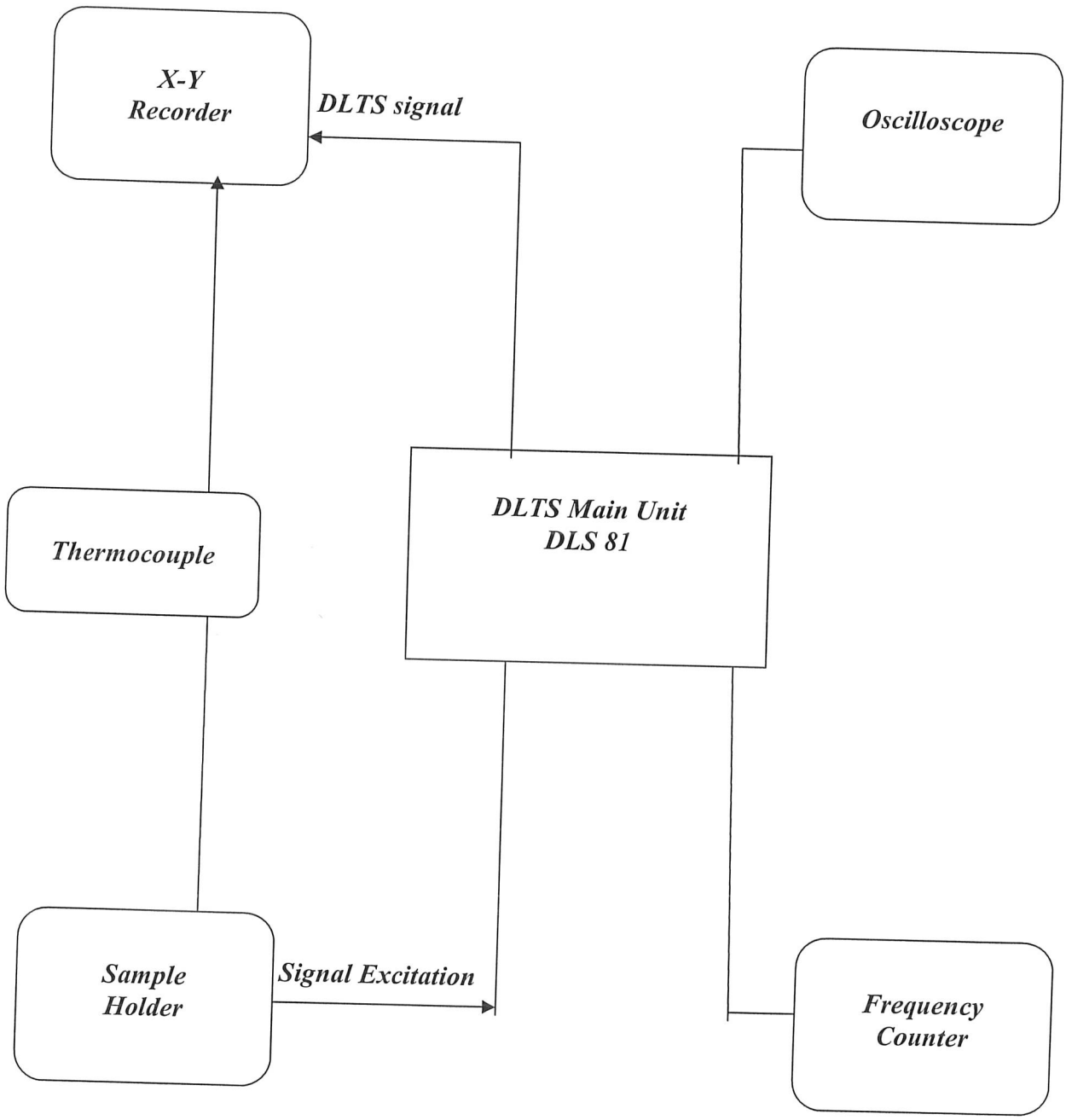

Fig.4.2 Block Diagram of " Deep Level Transient Spectroscopy" Experimental set-up.

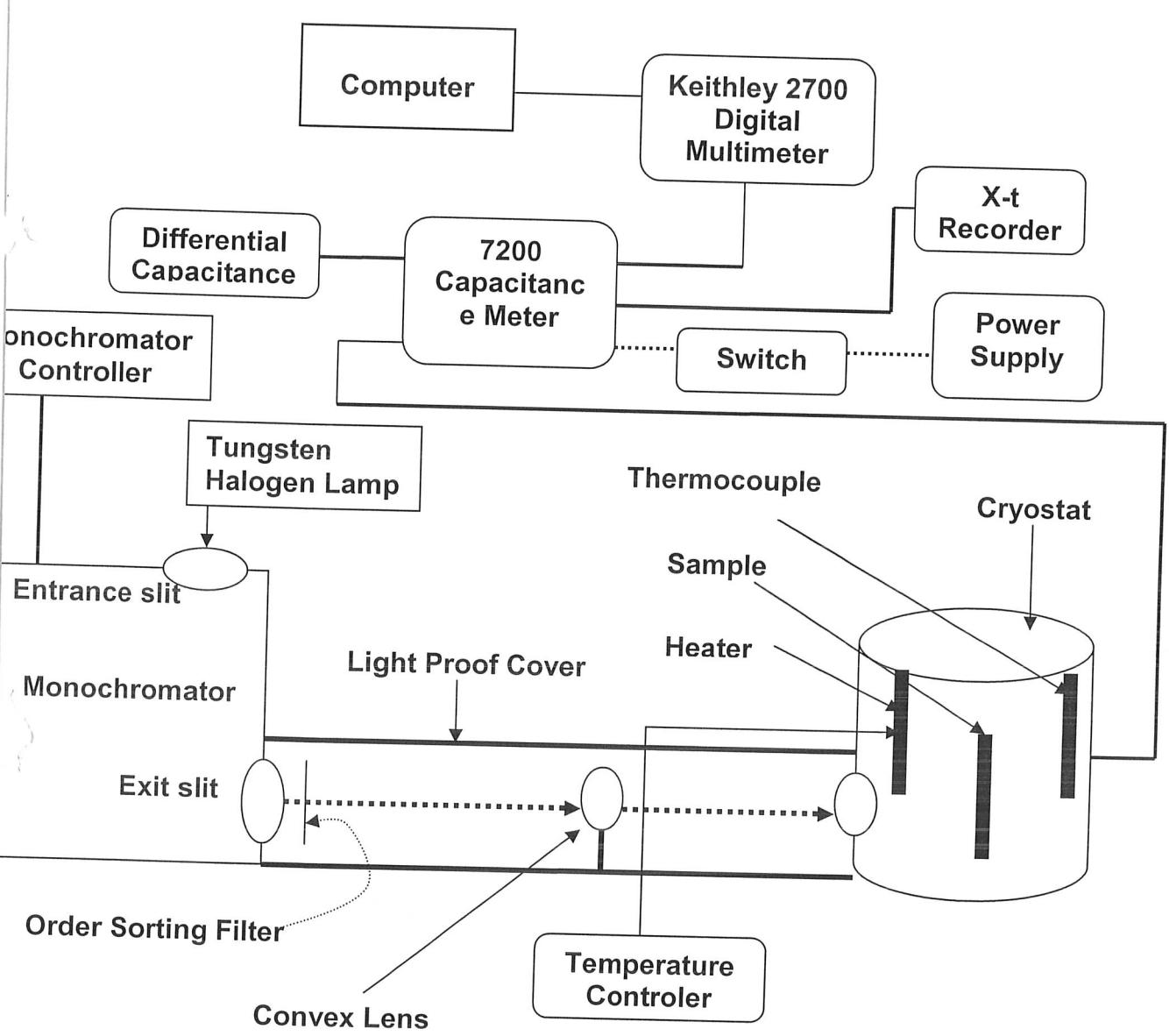

Fig. 4.3 Block diagram of Photocapacitance Experiment.

4.5 Temperature Control System.

In photocapacitance measurements, the stability of temperature is a crucial requirement. Thus a small change in temperature caused a significant change in output capacitance signal; therefore temperature had to be very stable. The system used to stabilize the temperature consisted of a cryostat, thermocouple and a micro-volt meter. The actual temperature of sample was measured with copper-constantan thermocouple. The thermo-voltage was measured by a Temperature controller TC-420. In our experiment the working temperature was only at 80K or at room temperature.

4.6 Light Unit

The light unit consists of 250 W, 24 V direct current tungsten-halogen lamps combined with a spherical mirror, which aims the high intensity of light at the mirror present behind the entrance slit of monochromator. To reduce the stray lights, the lamp unit is mounted in a metal case, with a lamp cooling fan. This light source provides a stable and easily aligned broad band source of visible radiation. This light source is ideal for general illumination, providing a smooth, continuous output from 190 nm to 2540 nm.

The lamp comprises of a tungsten filament in a quartz envelope containing halogen gas. The quartz envelope allows UV transmission down to 350 nm. The lamp is driven by a 25 A, 10 V power supply.

4.7 Optical Unit

The optical unit consists of a Spectra pro-500 monochromator with focal length of 500 mm and effective aperture ratio of f/6.9. The spectra pro-500 monochromator has three gratings of different number of grooves/mm and different blaze angles. The spectral range covers by using these grating are listed in table.

Grating (g/mm)	Wavelength rang (nm)	Energy range (eV)	Blaze Angle (nm)
1200	185-1400	7.20-0.89	500
600	185-2800	7.29-0.44	1000
300	185-5600	7.29-0.22	2000

"The range of grating used in spectra pro-500 monochromator"

The block diagram of Spectra pro-500 monochromator is shown in Fig.4.5. The instrumental arrangement consists of a Czerny Turner spectrometer, with variable entrance and exit slits from 10 um – 3.0 mm. The radiation transmitted through the entrance slit is collimated and directed towards the diffraction grating by a collimating mirror. The diffraction grating disperses the incident light radiation and this dispersed light falls on the focusing mirror, which direct and focus it on the exit slit. The band of wavelength can be calculated by suing the relation.

Reciprocal Linear Dispersion X Slit Width = $\Delta\lambda$

From the given wavelength 'λ' energy can be calculated by suing the relation

$$E\ (eV\ ) = \frac{1.23985}{\lambda\ (nm\ )} \times 10^{3}$$

4.7.1 Optimization of Light Focusing

Before staring the photocapacitance measurements, it was necessary to optimize the focusing of light onto the sample. This was accomplished by monitoring the photocurrent generated by the GasAs p+n sample when band-gap light (870 nm) was focused on it. The entrance and exit slits were both kept at 1mm during the experiment. The photocurrent was maximized by adjusting the focusing lens height and distance from the sample mounted in the cryostat. The maximum current observed was ~ 1.71 μA. During subsequent experiment, the focusing was checked periodically and adjusted if required.

Photocurrent measurements were performed at two different temperatures (room temperature and 80 K). An optical filter F5 with transmission range for first order from 715 nm to 1430 nm was used in the experiment.

4.8 Order sorting filters

According to Brag's law, for particular position of reflection grating, any incident wavelength λ is reflected at an angle 'θ' corresponding to different orders of 'n'. This means that any described setting of wavelength at input contains in additions to the first order of required λ, second order of $\lambda/2$, third order of $\lambda/3$ and so, when continuous light source is used

$$2d \sin\theta = n\lambda$$

To suppress these higher orders of wavelengths, order sorting filters are used.

4.8.1 Oriel Short pass filters

A short pass filter allows all the wavelengths shorter than the particular wavelength (cut-off λ) and blocks al $\lambda > \lambda_{cut\text{-}off}$. The transmission of filters at $\lambda_{cut\text{-}off}$ is 50% and is 85% in the region below the cut-off wavelength. In our experiment we used the Oriel filter of different energy ranges in the energy region less than Eg/2. The wavelength and energy of these filters is given in table

Filter No.	Wave length (nm)	Energy (eV)
57930	5600-3875	0.22-0.32
57920	4592-2755	0.27-0.45
57910	3024-1722	0.41-0.72

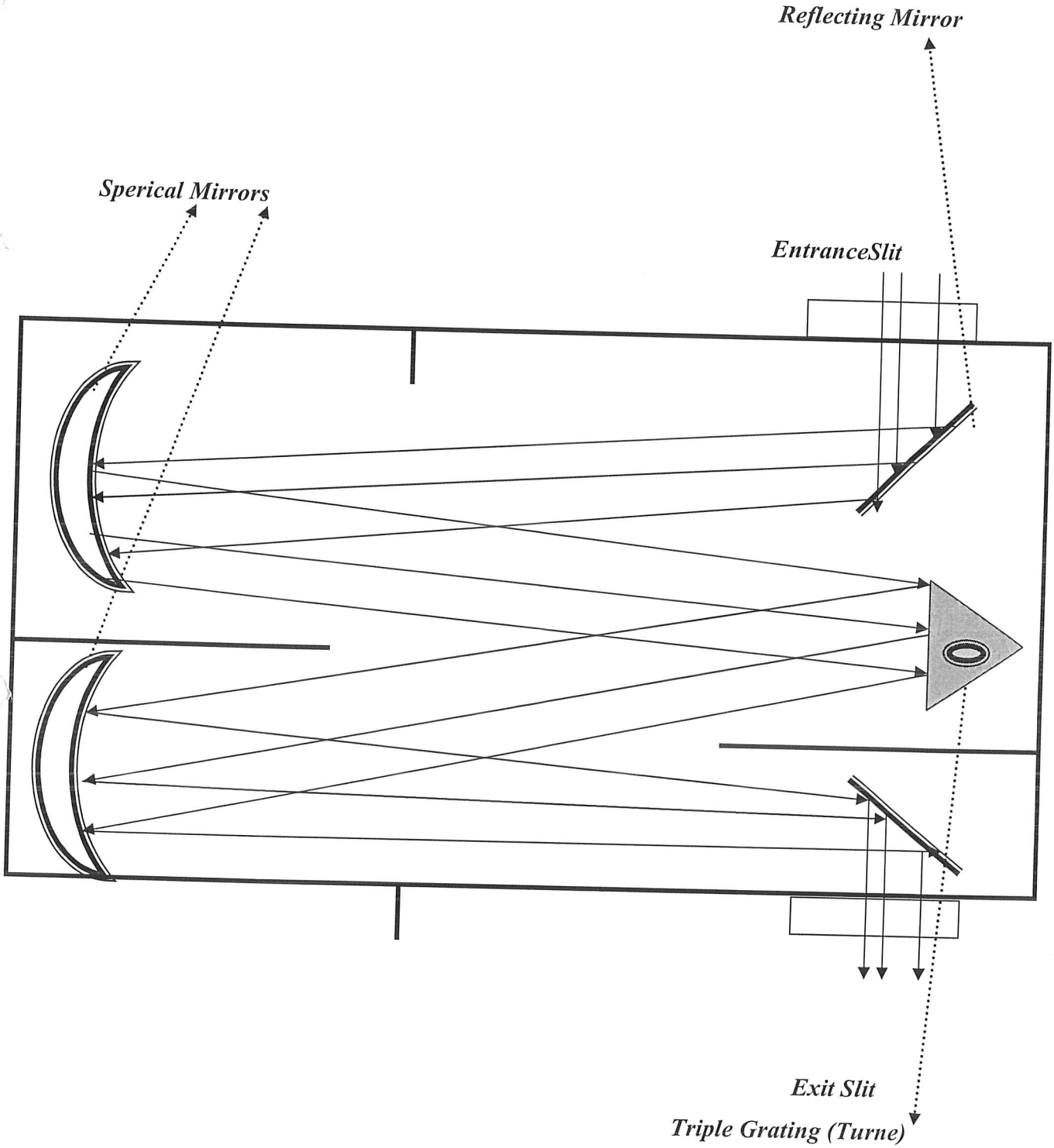

Fig. 4.4: ***Block Diagram of Spectropro-500 Monocromator***

Along with all these filters, we have used some other Filters for this purpose, such as COLOR FITERS (26-3319 and 26-3350). These Filters are made from high quality; normally have size 50.8 × 50.8 mm, and thickness about 1.0 mm. The range of wavelength from 1750 nm (0.70 eV) to 1150 nm (1.07 eV) has been covered by the combination of two filters, mentioned above (24-3319 and 26-3350).

4.9 The unit of Capacitance measurement

The measurement unit consists of DC power supply, Boonton 7200 capacitance meter. Voltmeter parallel to capacitance meter is used for constantly monitoring the output voltage of cells. A differential capacitance meter is also used along with Boonton 7200 capacitance meter, which enable us to measure the small capacitance change of the device with accuracy. The resolution of capacitance meter is $5x10^{-3}$ pF of full scale on all the ranges and its response time is 1 micro second. The output of change in capacitance due to electron/hole emission is recorded and also on x-t recorder.

4.10 Flux Measurement

The absolute values of photoionization cross-sections can only be calculated from optical emission rates, if the absolute values of photon flux are known.

A Hilger-Schwarz thermopile detector having SiO_2 window was used for flux measurement. The output signal was the voltage generated by the light falling on it. For DC voltage measurement of its output, a Keithley micro voltmeter model-155 was used. For each photon energy the flux was measured with the same slit width for which capacitance transient were taken, at a room temperature.

The measurements of the flux of light for different photon energies were done by using the thermopile. The thermopile used; having an area of 2 x 0.2 mm^2 had a stated

DC responsitivity of $\frac{40\mu volts}{\mu watts}$. For DC operation, a digital voltmeter was used giving output in microvolt.

The responsitivity of 1 μV are arose from 1/40 μwatt of incident power

1μV response was by incident power = $\frac{1}{[40\times1.6\times10-^{19}]}$ eV/sec

$= 1.56x10^{11}$ev/sec

flux = (incident power) (light energy shone x area)$^{-1}$

for 1μV signal, flux $\Phi = (1.56 \times 10^{11})\ [h\nu \times .004]^{-1}$

$$= \frac{3.9\times10^{13}}{h\nu} \times [\text{signal in } \mu V]$$

Chapter 5

Result and Discussion

This chapter describes the results of photocurrent and photocapacitance measurements carried out on GaAs n^+-p junctions, followed by discussion of results. Conclusions of work carried in this thesis have been summarized at the end of this chapter.

5.1 Reassembling of the set-up

Initially the experimental set-up for the photocapacitance transient technique was not assembled. Although this experiment was carried out in this lab some year before but when we started the work, all the set-up was dismantled. First of all the set-up was reassembled for experiment. It consists of number of sub units as follows:

5.2 Electrical Measurements

Before doing photocapacitance measurements, it is necessary to ascertain the device quality and also obtained information such as doping concentration , type of junction, deep level content etc. These information can be found from electrical measurements described below.

5.2.1 I-V and C-V Measurements

The I-V measurements of the sample were performed at room temperature at reverse bias upto 8V. The value of leakage current was found to be 1.04μA at V_R = 8V, which indicates that the sample is of good quality for present studies. I-V characterization of the sample is shown in Fig.5.1

The C-V measurements of the sample were performed at room temperature shown in Fig. 5.2 (a). The sample was found to be step junction type from the $1/C^2$ versus V_R plots, as shown in Fig. 5.2(b). The doping concentration obtained from this plot was 3.47E16, while the built-in voltage was found to be 1.15 V.

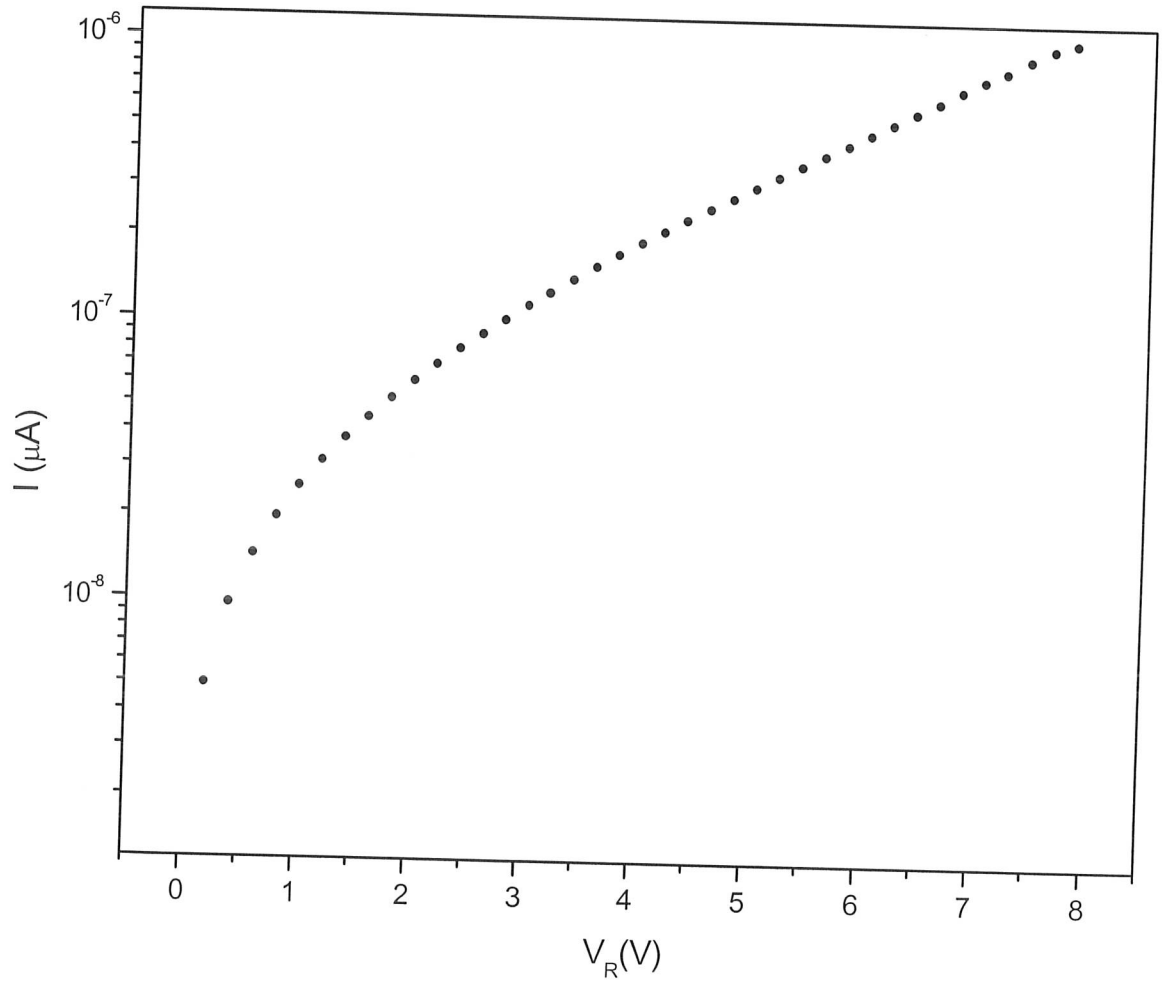

Fig. 5.1: ***I-V Characteristic Plot of GaAs.***

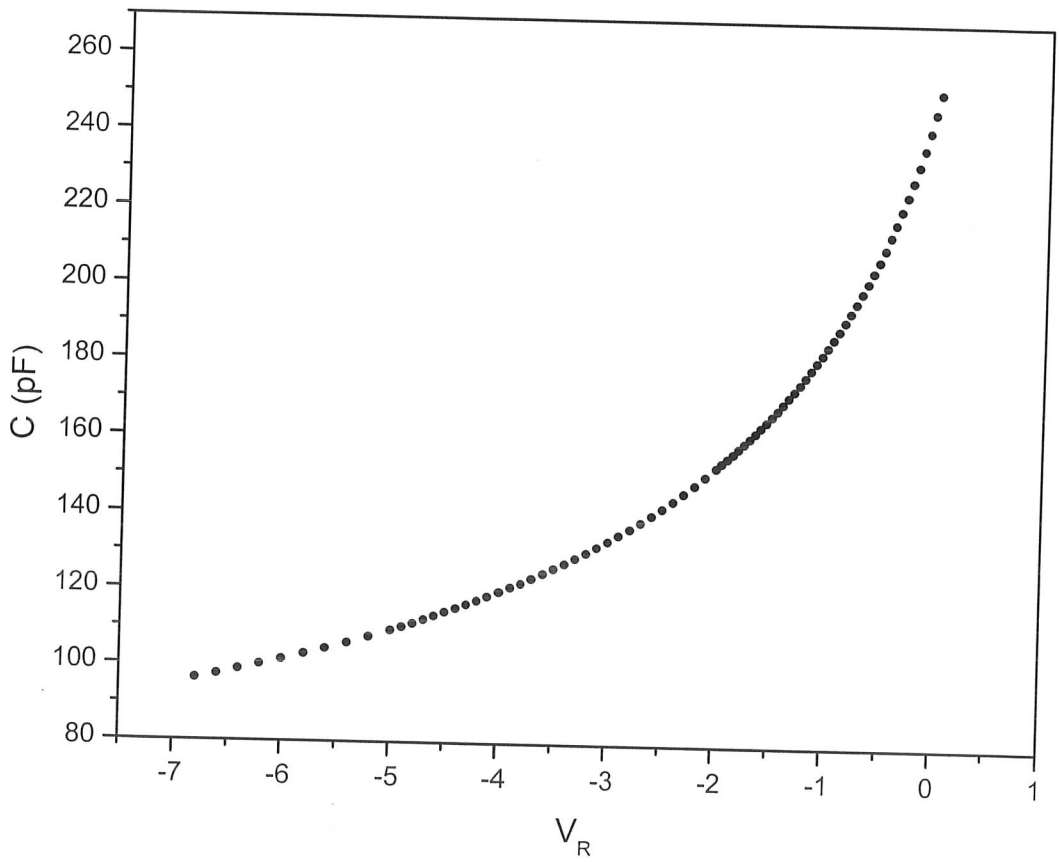

Fig. 5.2(a): C-V Characteristic Plot at Room Temperature.

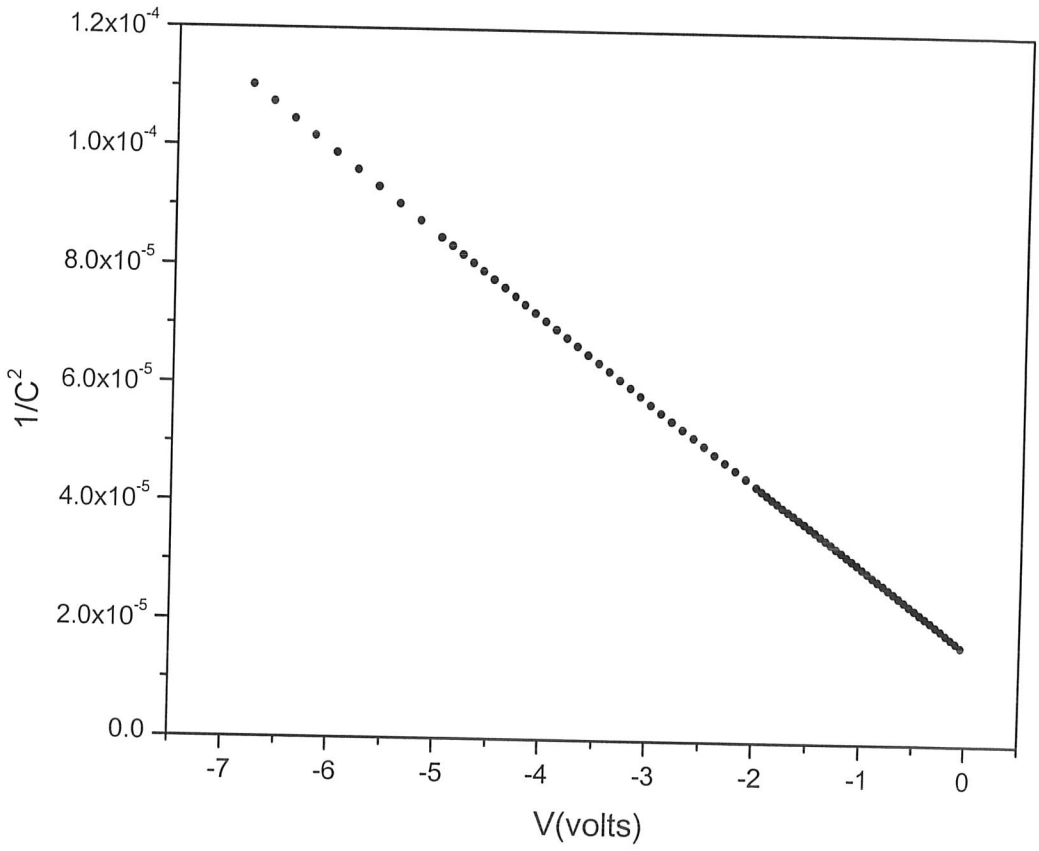

Fig. 5.2(b): $1/C^2$ vs Voltage Plot.

5.2.1.1 DLTS Measurements

Deep level transients spectroscopy was carried out on the sample as described in chapter 4, to detect the presence of deep levels in the sample. The measurements were done in the temperature range ~80k to ~350k. A typical majority carrier emission spectra is shown in Fig. 5.3. One electron emitting deep level was observed with the emission rate 100Hz at 270K having activation energy 0.54eV. It is the same level HM1 as observed in previous studies carried out in this lab. [1]

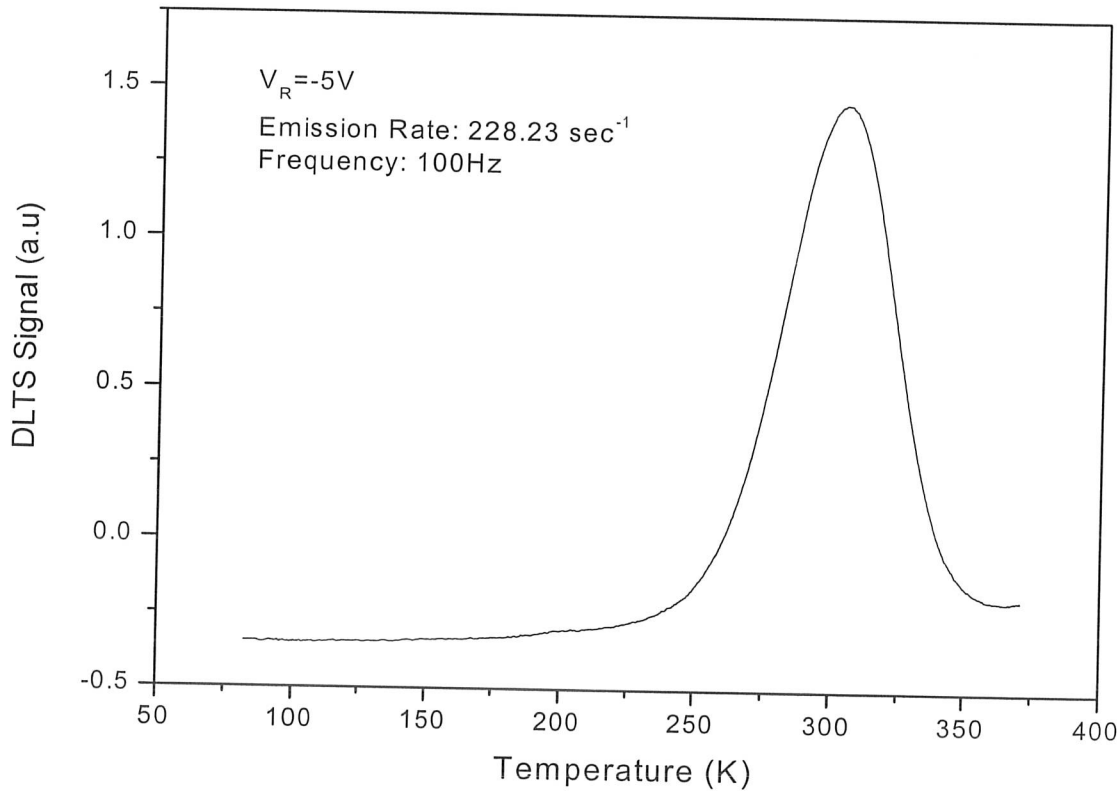

Fig 5.3 ***Majority carrier (holes) emission DLTS spectra.***

5.2.2 Interpretation of the electrical measurement

The I-V and C-V measurement of sample indicates that the quality of the sample is good for photocapacitance experiment. The DLTS spectra of the sample reveal the presence of majority (holes) level at activation energy ~0.54eV from conduction band, which is the activation energy of HM1 level **[1].** This level is co-related with the well known EL2 level in n-type GaAs **[3] [4] [5].** The emission rate signature is shown in the Arrhenius plot in Fig. 5.4

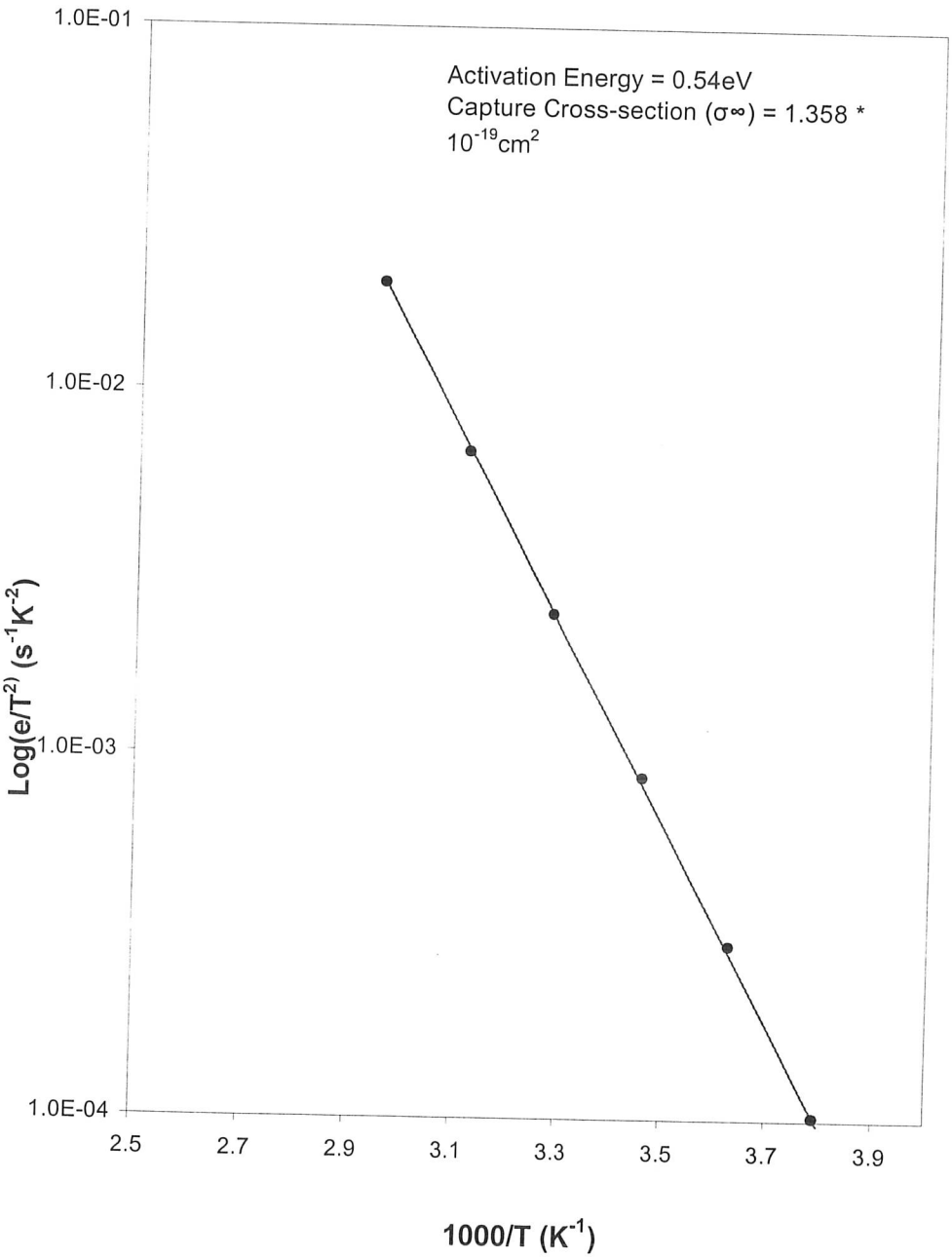

Fig. 5.4: Arrhenius plot of deep level.

5.3 Optical Measurements

5.3.1 Photocurrent Measurements

Initial condition: Switching bias (0 to -3V)

Photocurrent measurements were performed at two different temperatures (room temperature and 80K) by setting initial condition switching reverse bias from 0 to 3 V. An optical filter F5 having transmission ranges for first order from 715nm to 1430nm was used in this experiment.

Room Temperature measurements

Photocurrent experiment was performed at room temperature, small peaks was observed from ~0.70 eV to ~ 1.14 eV energies. An abrupt increase in photocurrent was observed at 1.42eV, which is the band-gap of GaAs at room temperature. On increasing the incident photon energy beyond 1.42eV, instead of increasing the photocurrent start decreasing and became very low at photon energy at photon energy 2.1eV. The plot of photocurrent (I_p) as a function of photon energy ($h\upsilon$) is given in Fig. 5.5(a).

Low Temperature measurements

The same experiment was repeated at low temperature (80K). The plot of I_p as a function of $h\upsilon$ at 80K is given in Fig. 5.5(b). The essential features remain same as observed at room temperature except that maximum photocurrent was now observed at 1.44eV.

Interpretation of Photocurrent Spectra

5.3.1 (a) Room Temperature

The room temperature photocurrent data exhibits the small peaks observed from ~0.70 eV to ~ 1.14 eV energies as shown in *Fig. 5.5(a)*. This range of energy lies in the range where the filter starts transmitting second and higher orders. Therefore, this increase in photocurrent could be attributed to contribution of higher order of near band-gap light. The second possible factor for these peaks may be due to the current generated tough two-step process via some deep level.

The photocurrent began to increase after 1.28eV. This increase in photocurrent is due to an increase in generation of electron-hole pair. The maximum photo current was observed at 1.42eV, which correspond to the band-gap of GaAs at room temperature. On further increasing incident photon energy, the photocurrent began to decrease instead of increasing. This decrease in photocurrent was due to the increase in absorption coefficient. By further increasing the photon energy, photocurrent dropped to zero because now at these energies light can only penetrate in a very thin layer of the sample and does not cause electron-hole pair generation.

5.3.1 (b) Low Temperature (80k)

When the measurements were taken at 80K, the maximum photocurrent was found to shift to the energy ~1.44 eV. This is due to the increase of the band-gap at low temperature. This increase in photocurrent is due to decrease in lattice vibration and collision processes. Decreased inter atomic spacing increased the potential seen by electrons in the material, which in turn widen the size of energy ban gap **[1].**

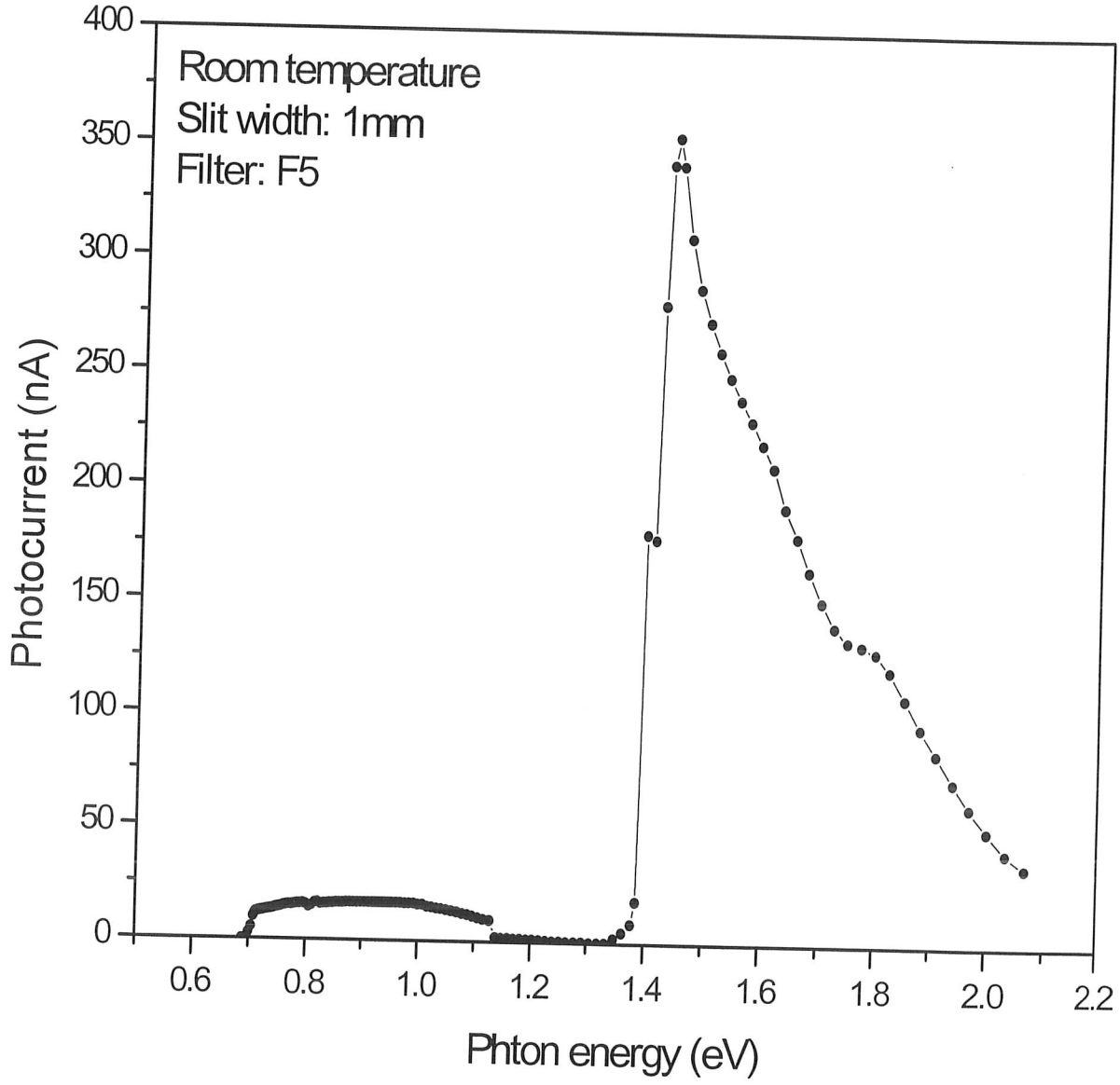

Fig. 5.5(a): Photocurrent Spectrum at room temperature.

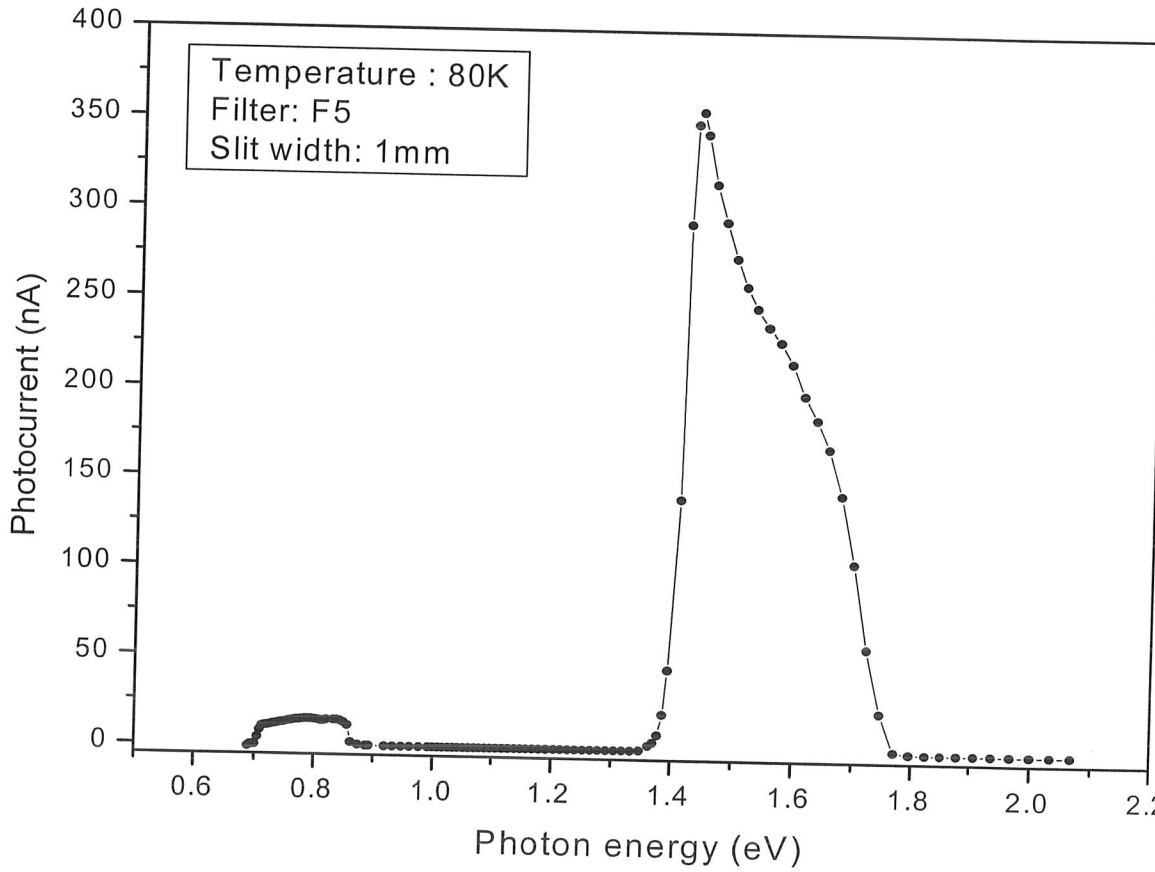

Fig. 5.5(b): Photocurrent Spectrum at low temperature (80K).

5.4 Photocapacitance Spectra *(ΔC vs hν)*

Here we describe the photocapacitance measurement in which change in capacitance ΔC corresponding to different photon-energies was recorded. The photocapacitance measurement was also performed at two different temperatures (room temperature and 80K). The initial condition (switching the bias from 0 to 3V) was applied before each *(ΔC, hν)*. Range of photon energy was covered from .022eV to 1.30eV in this experiment.

Room Temperature measurement

The photocapacitance measurement was performed at room temperature by using the initial condition switching the reverse bias from 0 to -3V. Photon energy from 0.22eV to 1.30eV has been examined with the difference of 0.1eV It was found that thermal emission transient was observed which was allowed to saturate before shining the different photon energies. The ΔC versus $h\upsilon$ data obtained is plotted in Fig.5.6. In the photon-energy ranging from 0.64eV to 0.71eV, no change in capacitance was observed. But from 0.71eV to 0.88eV, the capacitance decreases to minimum and remains almost constant till 1.06 eV, and then again it starts increasing. When it approaches to 1.10eV, it again starts decreasing and became minimum at 1.30eV.

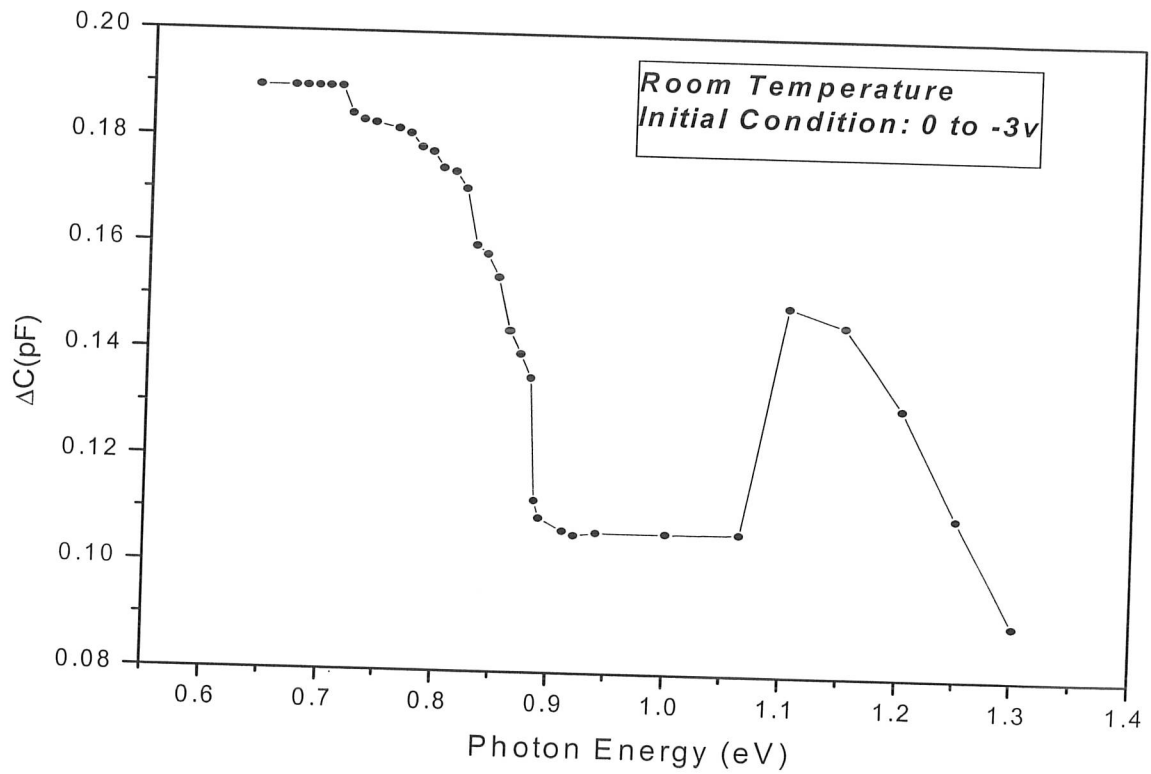

Fig. 5.6(a): Photocapacitance Spectrum at room temperature

Low Temperature measurement

This experiment was performed at low temperature (80K) with the same condition for room temperature measurement, i.e. initial condition of switching from zero to reverse bias of -3V. The ΔC versus hυ data thus obtained is plotted in Fig. 5.7. The energy range covered in this experiment was from 0.53eV to 1.30eV, by using the set of different filters. But the first transient was observed at The transmission range covered by the combination of these of filters used in our experiment is from 0.55eV to 0.71eV for Oriel filters, 0.71eV to 1.07eV for Color Filters (combination of 26-3319 and 26-3350) and 0.68eV to 1.73eV for an order sorting filter F5.

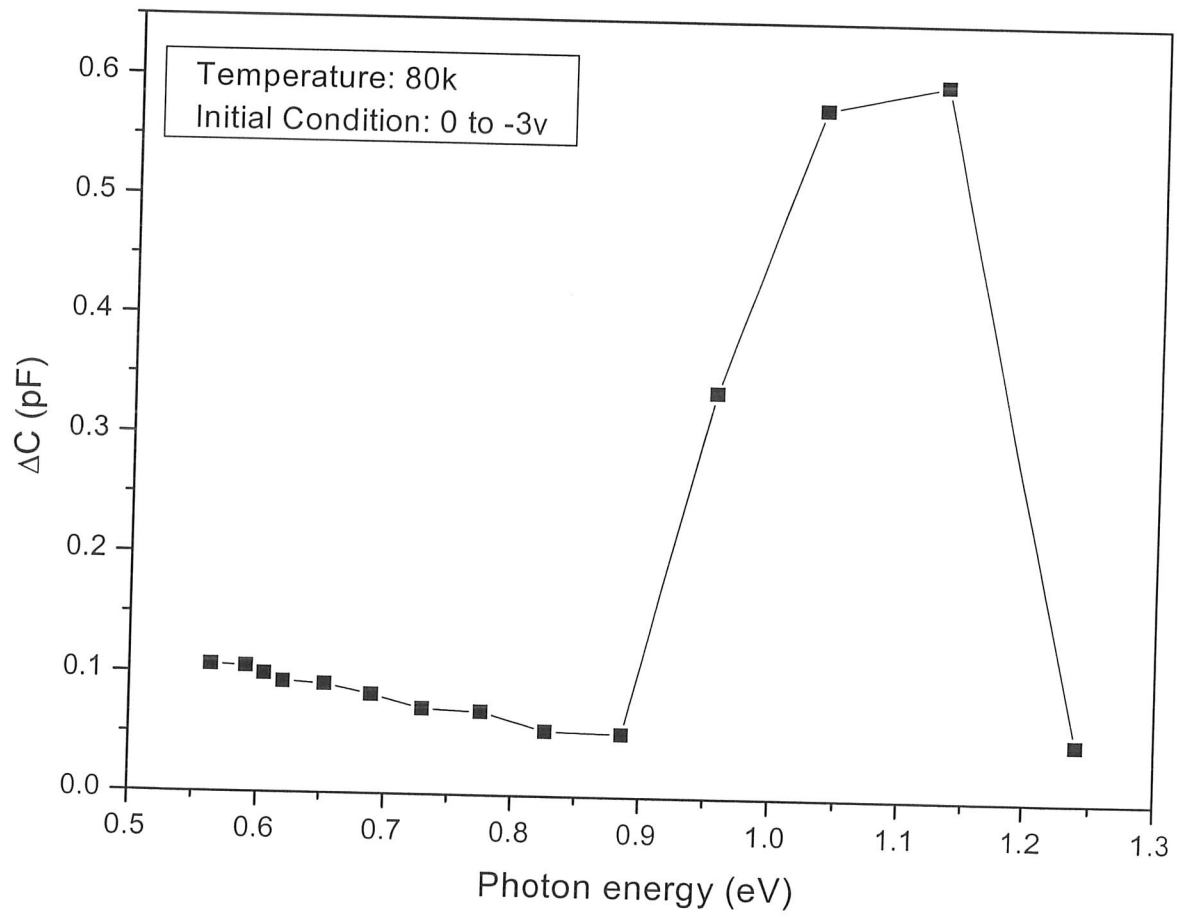

Fig. 5.6(b) Photocapacitance Spectrum at low temperature(80k).

5.4.1: Interpretation

Room Temperature interpretation

For the room temperature measurements described above, immediately after setting up the initial condition (switching bias from 0 to 3V), a thermal emission transient was observed. By switching the bias holes (majority carrier) are injected and all deep level within the band-gap would capture them. If enough thermal energy is available, these deep levels would thermally emit the carriers to the respective bands. This thermal emission transient was analyzed by plotting ln[ΔC] versus time, as shown in Fig 5.11 and 5.12. The slope of this plot gives the thermal emission time constant τ according to equation,

$$\frac{dn(T)}{dt} = \left(e_p^0 + c_n n\right)\left(N_{TT} - n_T\right) - \left(e_n^0 + c_p p\right) n_T$$

Here one must note that since the photon energy range covered is 0.55eV-1.30eV, both electron and hole emission process are possible. The negative change in capacitance showed that, for these photon energies hole emission process is dominant. By increasing the photon energy the electron emission process become faster and after 1.07eV, electron emission become dominant over hole emission. The magnitude of ΔC rapidly increased from the photon energy 1.07eV to photon energy 1.11eV and then it decayed back to lower side of ΔC. This change in ΔC corresponds the double transition.

Low Temperature Interpretation

Using the initial condition of switching from zero bias to -3V at 80KK causes the HM1 level to be filled with holes and to remain filled at low temperature. Thus the HM1 level is completely occupied at this temperature. Shining photons of different energy would now cause no electron emission process since all levels are filled holes, as long as HM1 remains filled. Thus one would expect ΔC to be very low (~0.05pF) for hν < ~0.89eV, which was exactly what was observed. At 0.60eV positive ΔC was observed which initially decreased as the photon energy was increased and then beyond 0.89 eV, it

increased {Fig. 5.6(b)}. This increased in magnitude continued till ~ 1.03eV after which it decreased and approaches to its minimum value at 1.24eV. Here again one must keep in mind the fact that we are in two-step process region for the photon energies > 0.89eV, which was exactly what was observed in previous studies carried out in this Lab while studying the deep level defects in n-type GaAs.

Thus the capacitance change in this region have both electron-emitting and hole emitting components. The decreasing trend of magnitude of ΔC from 0.58eV - 0.87eV could be attributed to either the, (a) interplay photoionization cross-section of electrons and holes or (b) actual hole emission from other deep level. The decrease observed after 1.03eV can be explained by the absorption of incident photons due to smaller penetration depth at these energies.

5.5 Optical Emission Rates

Bias switching (0 to -3V)

Capacitance transient at room temperature

Full capacitance transient corresponding to different incident photon energies of the photocapacitance spectra for the initial condition reverse bias switching from 0 to 3V were obtained at room temperature. Photon energy from 0.22eV to 1.30eV has been examined with the difference of 0.1eV by using the appropriate set of filter as discussed earlier (section 5.4). Some full capacitances transient at room temperature are shown in Fig. 5.8 (a, b).

Capacitance transient at low temperature (80K)

Some full capacitance transients at 80K are shown in Fig. 5.9 (a, b, c). Here in this case different photon energies was incident on the sample, photon energy range has been examined from 0.53eV to 1.30eV with a random difference. The first capacitance transient was observed at photon energy 0.60eV which was small capacitance transient.

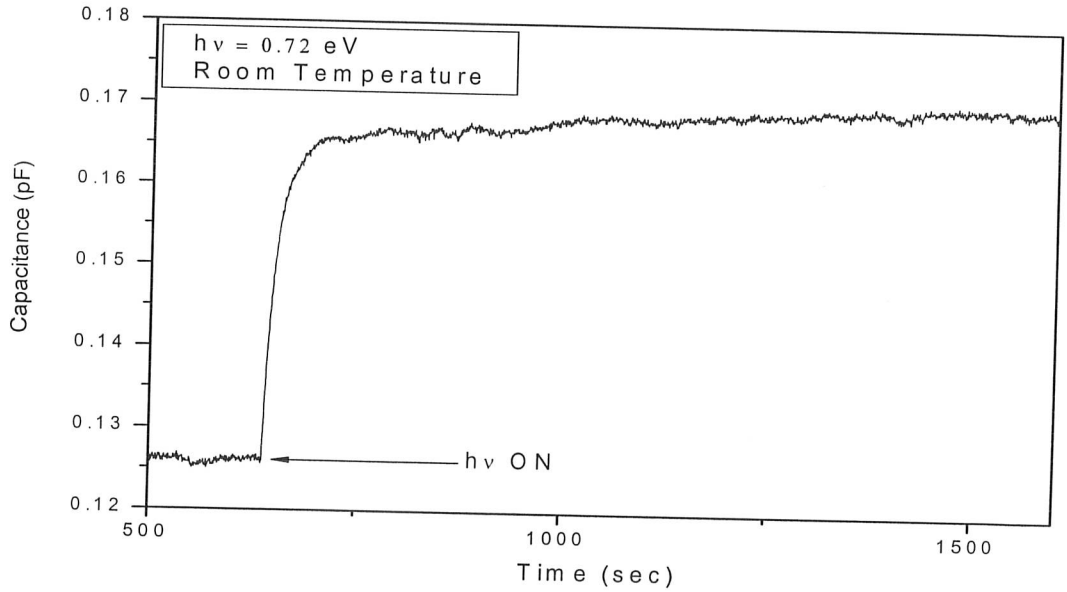

Fig. 5.8(a): Actual capacitance transient of photon energy 0.72 eV obtained at Room Temperature

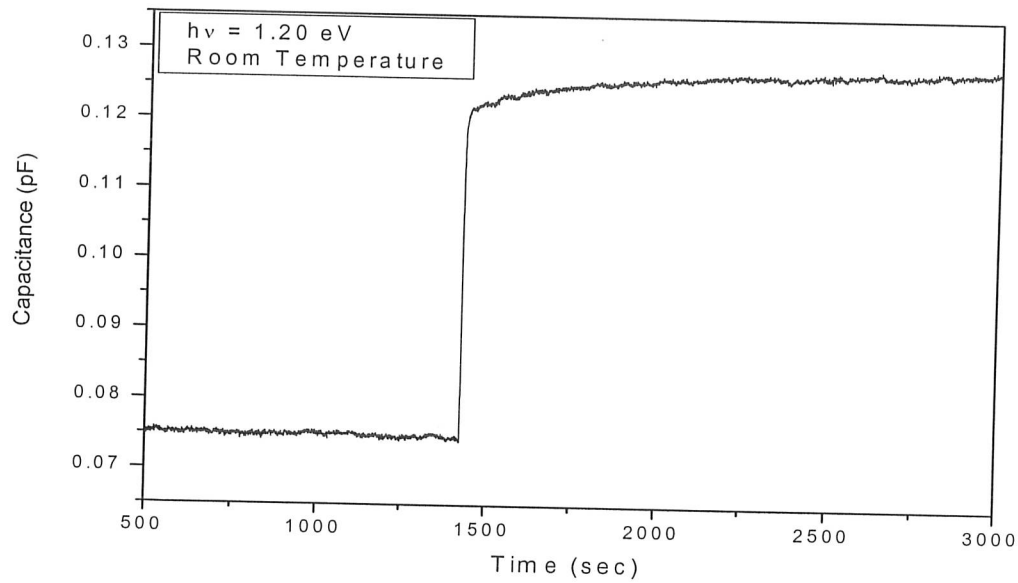

Fig. 5.8(b): Actual capacitance transient of photon energy 1.20 eV obtained at Room Temperature.

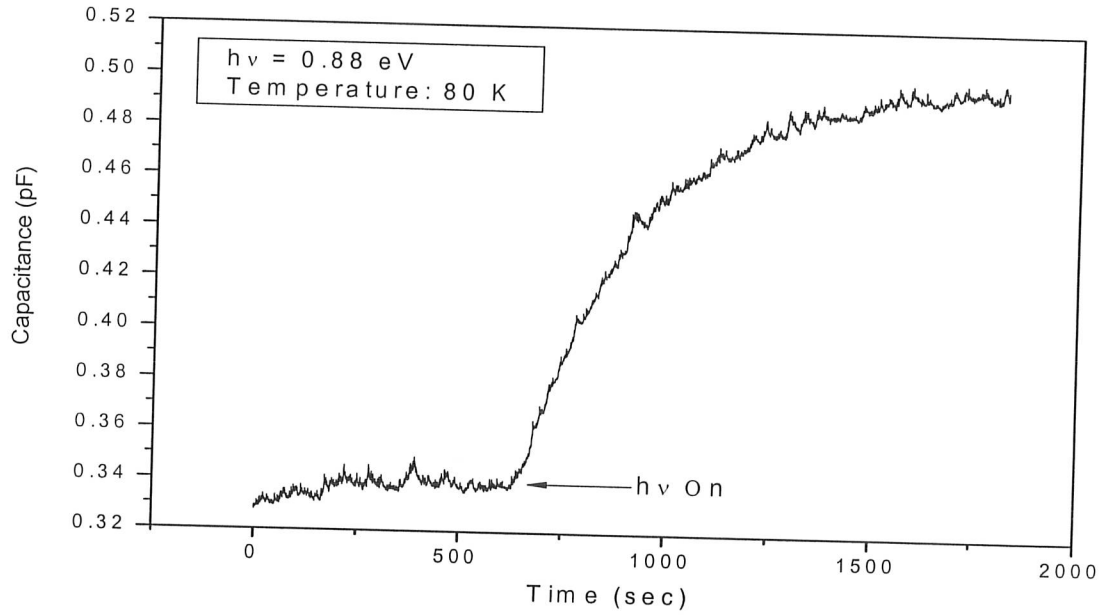

Fig. 5.9(a): Actual capacitance transient of photon energy 0.88 eV obtained at 80 K.

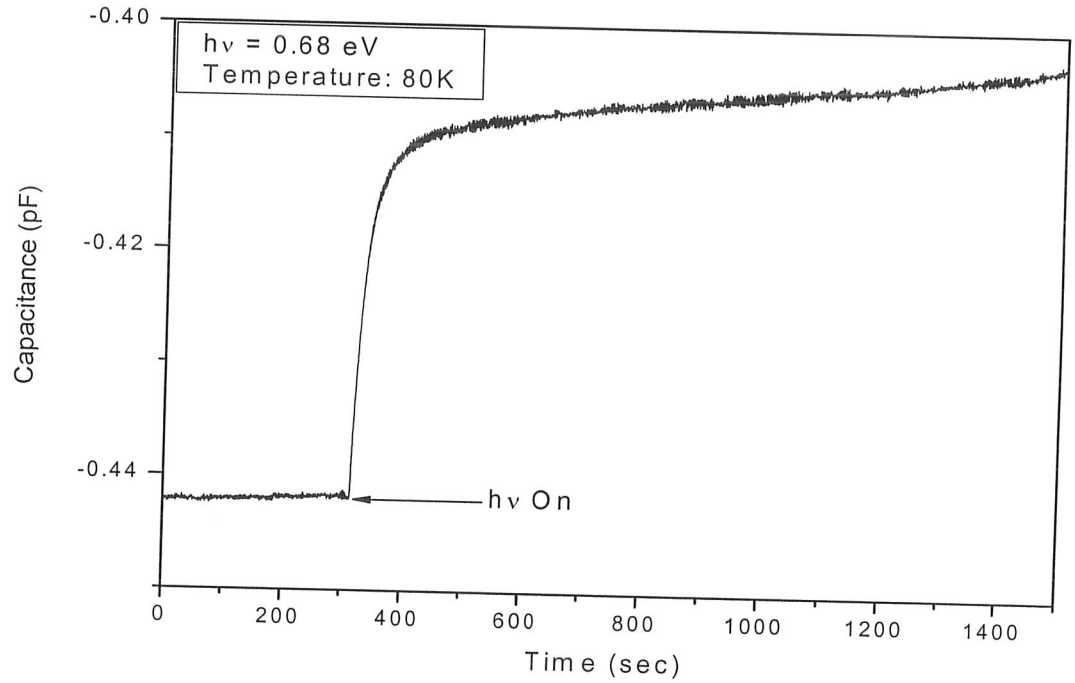

Fig. 5.9(b): Actual capacitance transient of photon energy 0.68 eV obtained at 80K.

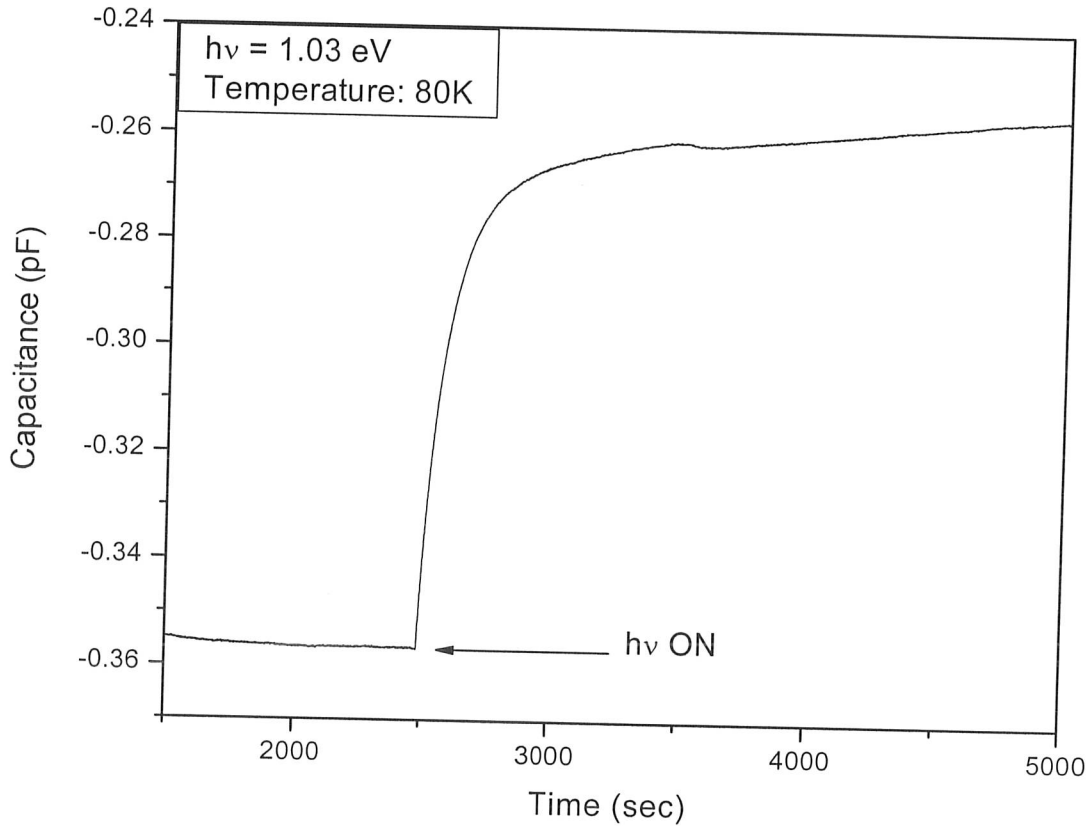

Fig. 5.9(c): Actual capacitance transient of photon energy 1.03 eV obtained at 80K.

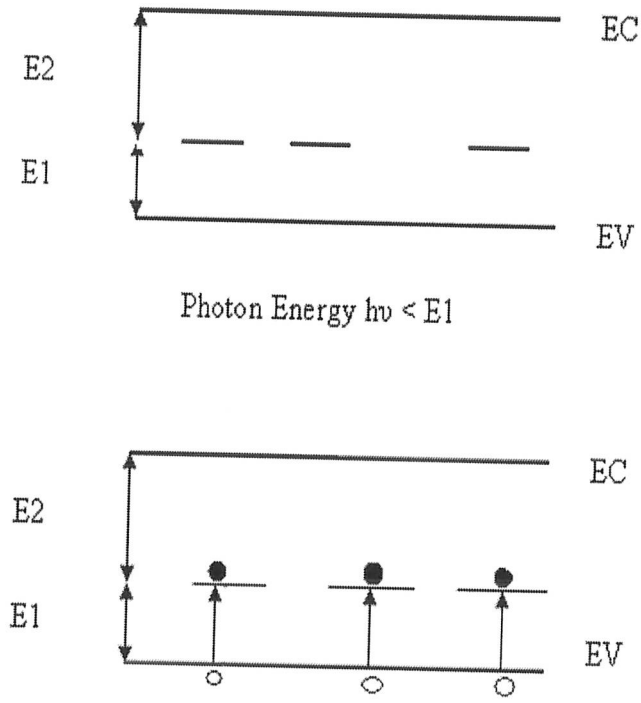

Fig. 5.10: ***Two-step process for hυ of different Photon energies.***

The change in ΔC as a function of time for some of the capacitance transients are plotted at room temperature and at 80 K. room temperature plots are shown in Figure 5.11 (a, b, c, d) low temperature plots are shown in 5.12 (a, b, c). The slope of the ln [ΔC] versus time curves gives the optical emission time constants (τ). Table 5.1 and 5.2 are corresponding the energy versus emission time constant at room temperature and at low temperature respectively.

Table 5.1: Energy vs. Emission Time constant at Low Temperature (80 K).

Energy (eV)	**τ (sec)**	**Energy (eV)**	**τ (sec)**
0.60	190.81	0.82	161.3
0.62	292.8	0.88	281.71
0.65	37.83	0.95	290.02
0.68	25.09	1.03	285.62
0.72	19.19	1.12	26.9
0.77	50.43	1.24	22.88

Table 5.2: Energy vs. Emission Time constant at Room Temperature.

Energy (eV)	τ (sec)	Energy (eV)	τ (sec)
0.67	18.52	0.84	19.73
0.68	23.03	0.85	18.24
0.69	17.12	0.86	18.66
0.70	25.2	0.87	26.57
0.71	19.84	0.88	20.56
0.72	21.88	0.89	18.76
0.73	15.83	0.90	20.55
0.74	15.11	0.91	16.63
0.75	11.51	0.92	18.69
0.76	12.4	0.94	16.63
0.77	14.14	1.00	14.58
0.78	14.39	1.06	19.94
0.79	17.33	1.10	2.147
0.80	14.63	1.15	2.888
0.81	12.32	1.20	2.375
0.82	16.57	1.25	2.4
0.83	19.63	1.30	2.485

5.5.1 Interpretation

Room Temperature and Low Temperature

As, at both the temperatures (room temperature and low temperature) different photon energies were made incident on the sample. The first transient was observed at room temperature was at 0.64eV photon energy and at low temperature at 0.60eV. If we talk about the room temperature the first small capacitance transient was small. Beyond 0.64eV all the capacitance transient was recorded with the difference of 0.1 eV. Before each capacitance transient the initial condition (bias switch from 0 to 3V) was set.

All the capacitance transients were obtained under this condition were rising transients, with no falling component appearing at any incident photon energy. Thus one can assume here that the hole-emission process (corresponding to negative change in capacitance) is either not present or much slower compared to the rising capacitance component (corresponding to electron emission).

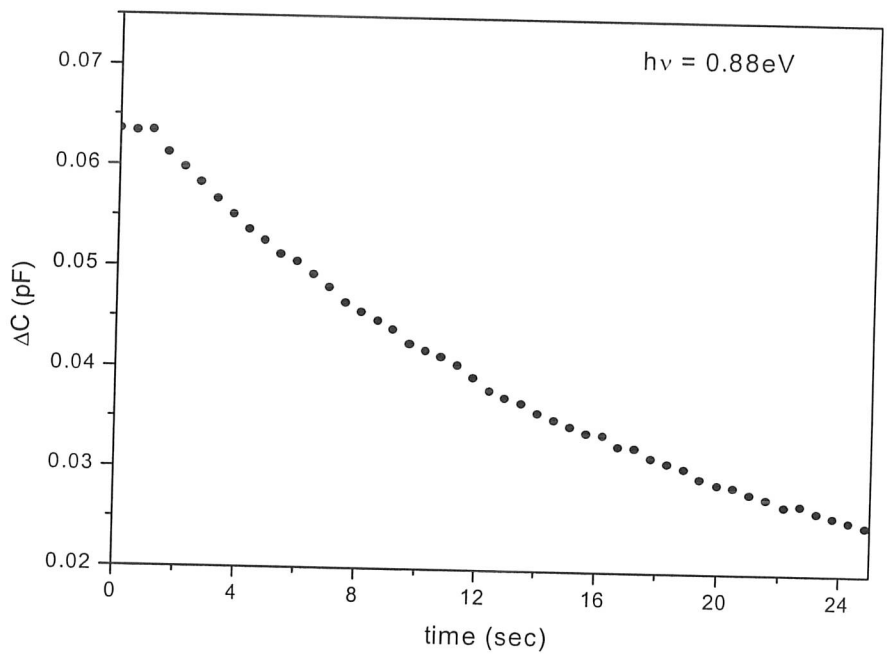

Fig.5.11 (a)

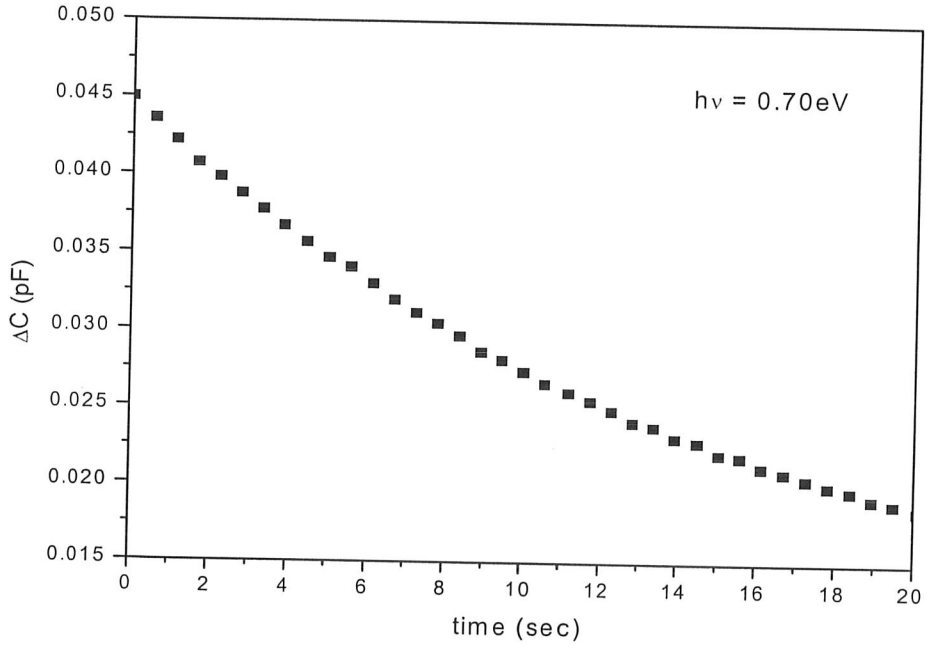

Fig.5.11 (b)

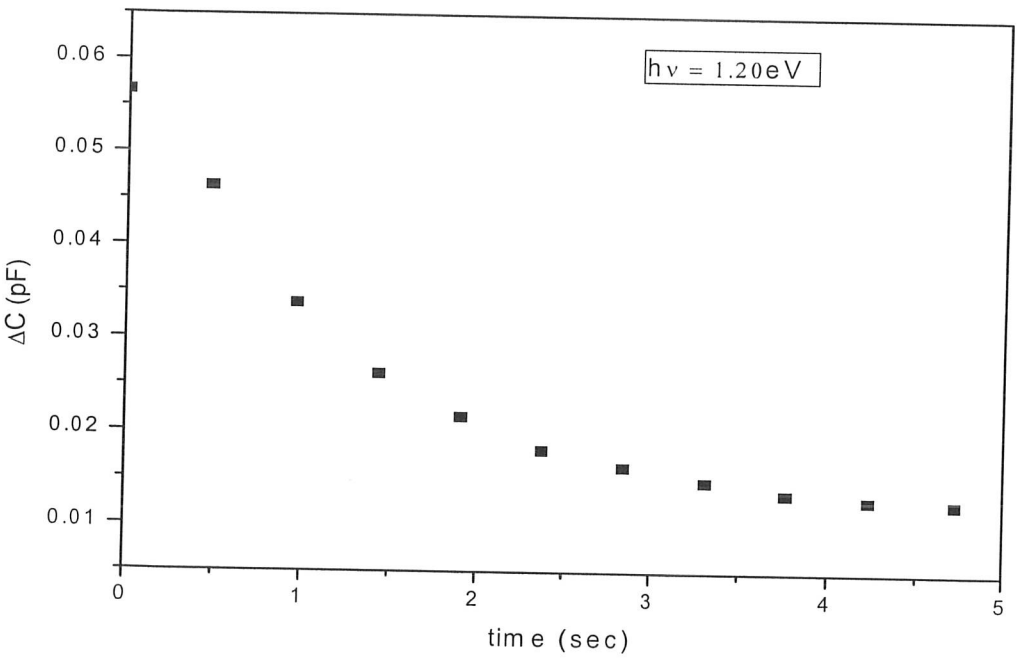

Fig.5.11(c)

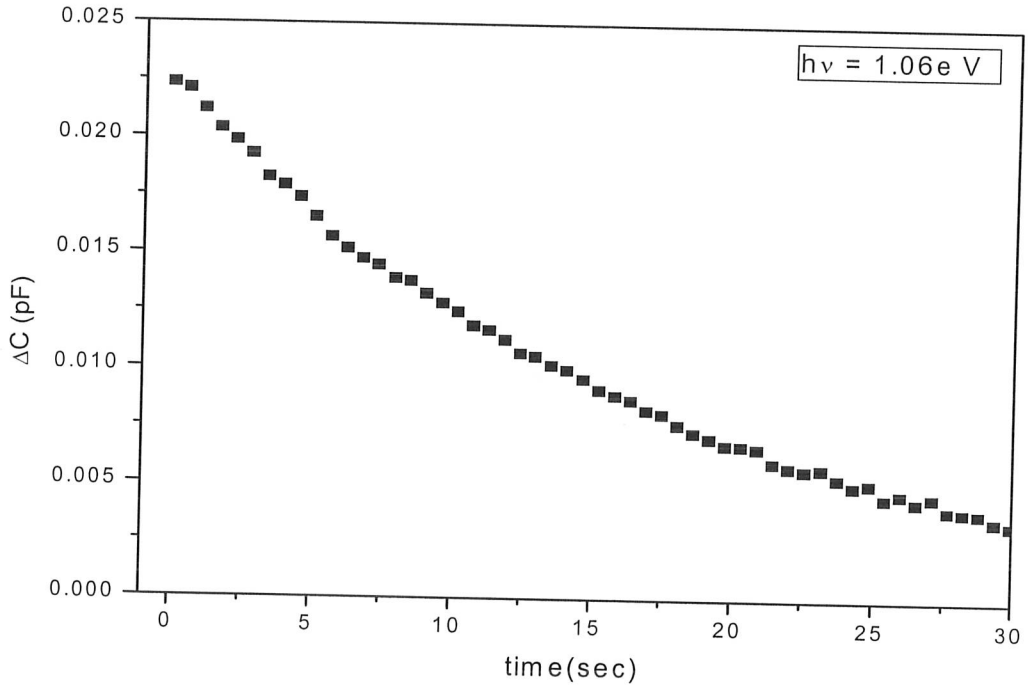

Fig. 5.11 (d)

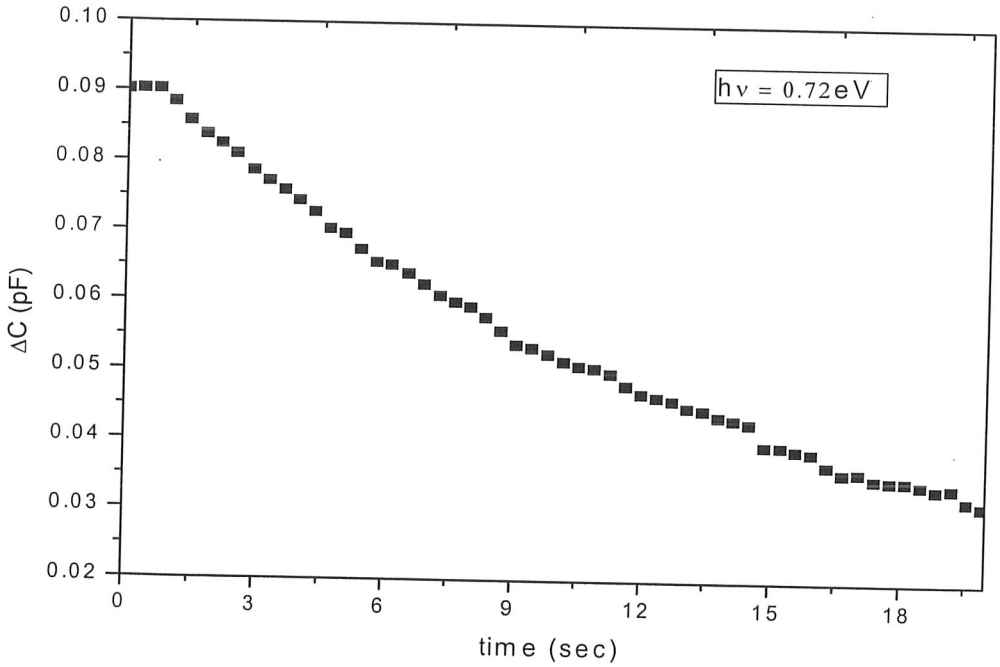

Fig. 5.12 (a)

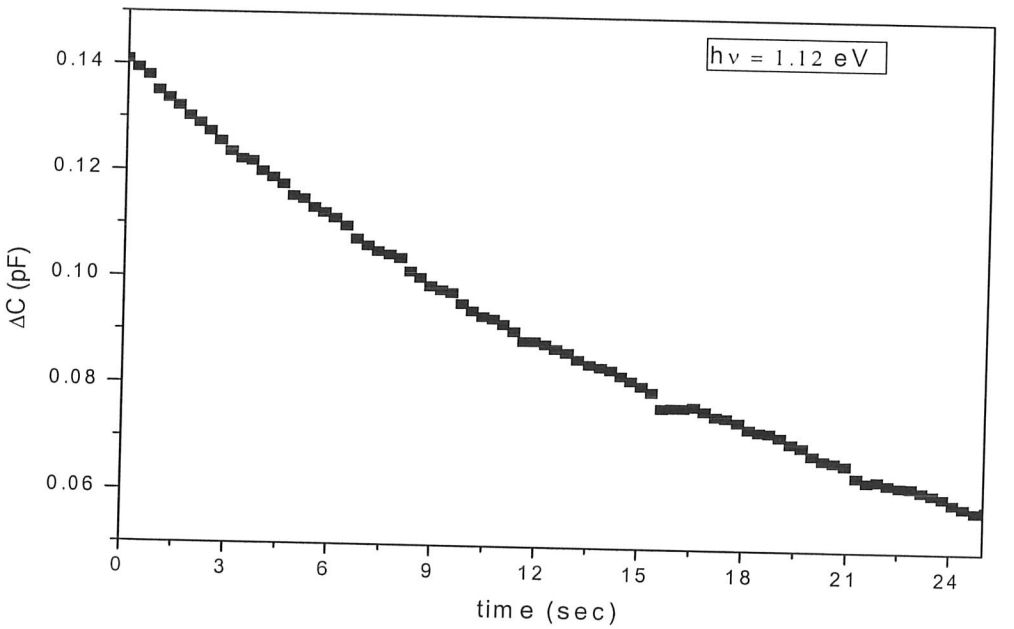

Fig. 5.12 (b)

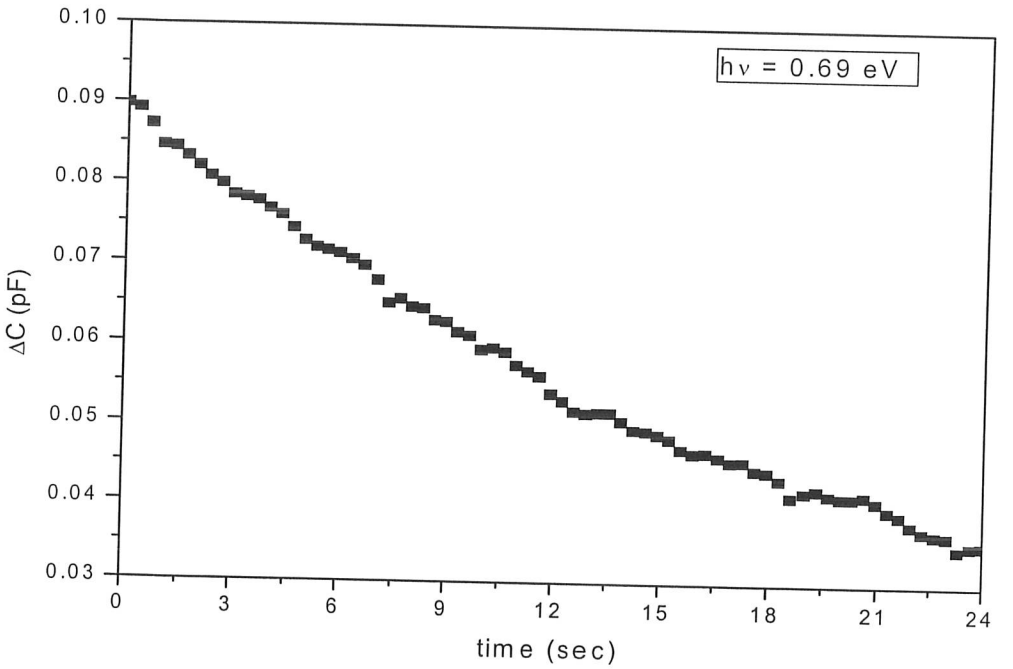

Fig. 5.12 (c)

5.6 Flux Measurement

The measurement of flux of light for different photon energies were done by keeping all parameters same, the same slit width and the same filters were used for which capacitance transient were taken An Hilger-Schwarz thermopile detector having SiO_2 window was used for flux measurement. Fluxes measured for each photon energy are given in table 5.3.

5.7 Photocapacitance Quenching

This experiment was done at 80K by using the initial condition (bias switching from 0 to 3V). In order to obtained the pure first order light, appropriate set of filters was used. Photons having the energy in the range 0.56eV to 1.30eV were made incident on the sample after setting up the initial condition. In this experiment initial set at room temperature. After setting up the initial condition the sample was slowly cool down to 80K by pouring the small amount of liquid nitrogen in cryostat. At 80K, light of different photon energies were made incident on the sample. A rising transient was observed, and it saturate almost. At this stage, by blocking the incident photon energy the capacitance slowly decayed and approaches its initial value. It was observed that rising transient saturated within ~ 60 seconds. Decay of the capacitance was observed to be much slower. Fig 5.13 showed that the capacitance has decayed to 85% of initial value in 53 minutes for the photon energy 0.88eV.

Table: 5.3. Flux measurements for different energies.

hν (eV)	$V_P(\mu V)$	Φ (Photons cm^{-2} sec^{-1})	hν (eV)	$V_P(\mu V)$	Φ (Photons cm^{-2} sec^{-1})
0.67	1.2	6.07×10^{13}	0.84	1.0	4.03×10^{13}
0.68	1.2	5.99×10^{13}	0.85	0.9	3.59×10^{13}
0.69	1.2	5.90×10^{13}	0.86	0.9	3.54×10^{13}
0.70	1.2	5.81×10^{13}	0.87	1.3	5.06×10^{13}
0.71	1.2	5.71×10^{13}	0.88	1.0	3.85×10^{13}
0.72	2	9.41×10^{13}	0.89	1.0	3.82×10^{13}
0.73	2	9.28×10^{13}	0.90	1.2	3.80×10^{13}
0.74	2	9.15×10^{13}	0.91	1.2	4.47×10^{13}
0.75	2	9.03×10^{13}	0.92	1.4	5.15×10^{13}
0.76	2	8.92×10^{13}	0.94	1.2	4.32×10^{13}
0.77	2	8.80×10^{13}	1.0	1.0	3.39×10^{13}
0.78	2.8	1.22×10^{14}	1.06	1.0	3.19×10^{13}
0.79	2.5	1.07×10^{14}	1.10	5.9	1.81×10^{14}
0.80	2.7	1.14×10^{14}	1.15	6.5	1.91×10^{14}
0.81	3.0	1.25×10^{14}	1.20	6.3	1.78×10^{14}
0.82	1.0	4.13×10^{13}	1.25	5.5	1.49×10^{14}
0.83	1.0	4.08×10^{13}	1.30	5.8	1.51×10^{14}

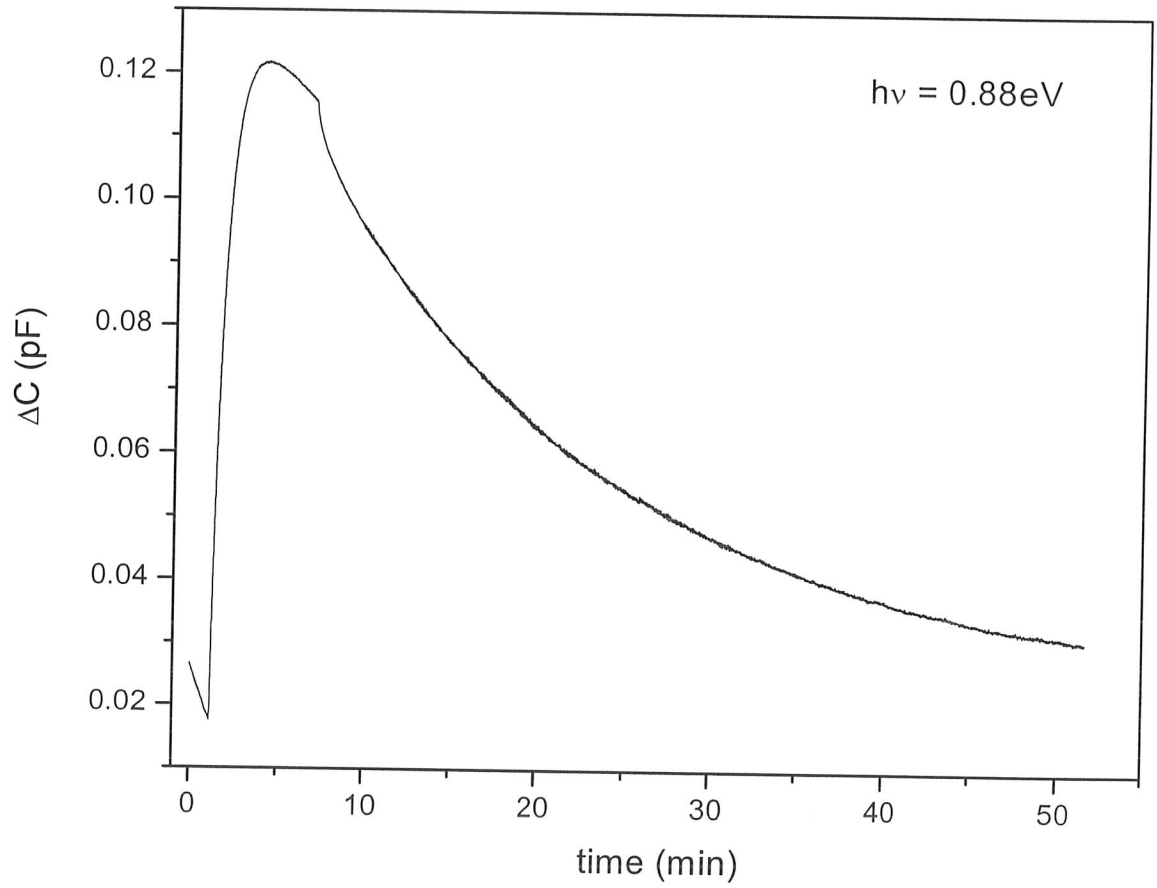

Fig 5.13: ***Photocapacitance transient observe with HM1 at 80K.***

Interpretation

At low temperature (~80K), one of the signature of HM1 level is photoquenching effect observed, may be associated with the transformation of EL2 into a metastable state HM1. Decay of capacitance after initially rising to maximum and come back to its initial value corresponds to the refilling of HM1 level. But, if HM1 level is filled, then switching off the light and then switching it on again should give a rising transient

corresponding to emission, however this is not observed and there is no or little change in ΔC.

5.8 Discussion of Photocapacitance Transients

In Fig 5.13, optical capture cross-section (σ°) versus photon energies were plotted. Here the optical capture cross-section $\sigma^\circ = \sigma^\circ_n + \sigma^\circ_p$ have been obtained by multiplying the flux (Φ) of incident photon energy with the emission time constant of the photocapacitance transient. In our experiment the photoionization cross-section is found to increase with incident photon energy. Emission probability exist for both electrons and holes in the present work. The photoionization cross-section thus obtained are more or less in agreement with published data [6]. However, the scatter observed can be accounted for the temperature instability.

5.9 Discussion of Photocapacitance Quenching

In our experiment, due to lake of temperature controlling system, temperature fluctuation was observed. This cause the capacitance of the diode to fluctuate causing an error in actual ΔC that was being measured. Due to rise of temperature, the capacitance would also increase and hense it would affect the saturation and decay of transient.

The emission rate obtained from the slope of the ln [ΔC] versus time curves were corrected for flux and resulting $\frac{1}{\tau\phi}$ was ploted as the function of photon energy as shown in Fig 5.13. As discussed above, due to temperature fluctuation our data is scattered and hence not accurately fit with the published work [7]. However, the photoquenching effects do prove the existence of the somehow same level in our sample, which is observed in [7].

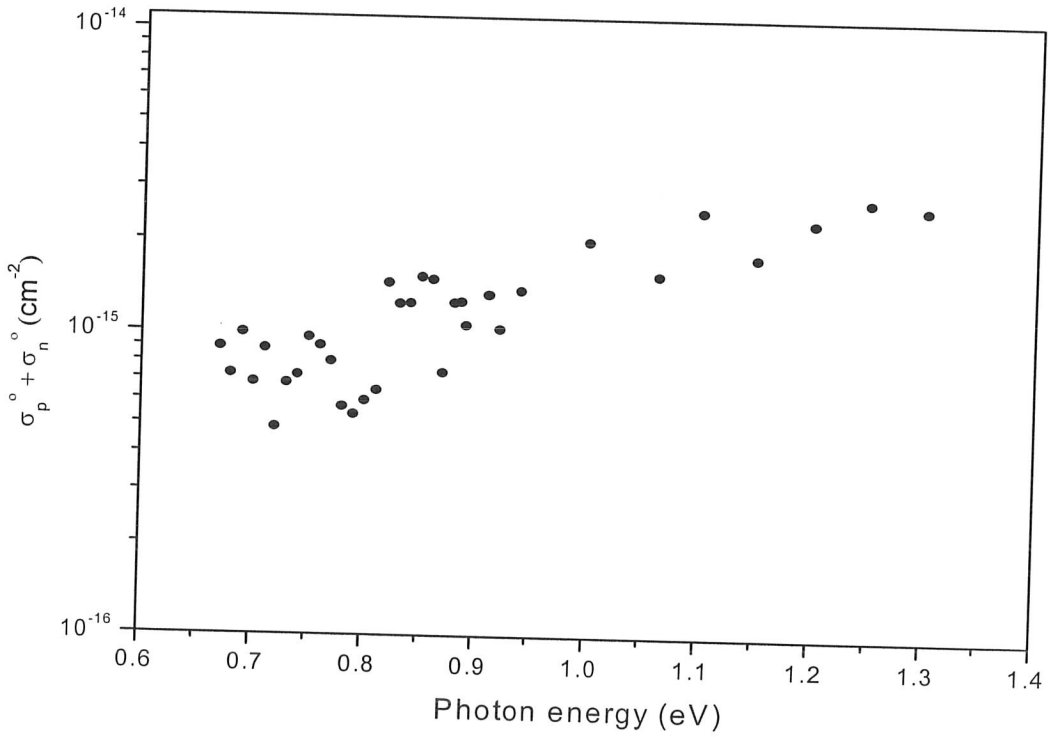

Fig. 5.13: Photoionizationation cross-section of HM1 at 80K obtained from the raising part of photocapacitance transient using 0 to -3V initial condition.

5.10 Conclusions

To summaries the presence work, two basic goals have been achieved. First the reassembling of all sub units of the photocapacitance technique and setting up both at room temperature and low temperature, has been achieved. Second, to use this set-up to measure the electron and hole photoionization cross-section. The technique has been tested on deep level defect HM1 in p-type GaAs and some optical properties of this defect have been taken. These measurements include photoionization cross-section (σ°_{n}) and the photo quenching effect.

Certain improvements in the set-up are required necessarly such as better controlling system for more accurate data and the better optical optimization.

5.11 References

1 Principle of semiconductor devices bt BART Vanzeghbroeck (2004).

2 Nazir. A. Naz, Umer. S. Qureshi and M. Zafar Iqbal, JAP 106,103704 (2009).

3 A. C. Irvine and D. W. Palmer , Phys. Rev. Lett. 68, 2164 (1992).

4 L. Samuelson and P. Omling, Phys. Rev B.34, 5603 (1986)

5 J. Dabrowski and M. Scheffler, Phys. Rev. Lett, 60, 2183 (1988).

6 P. Omling, L. Samuelson and H. G. Grimmeiss, Phys Rev B. 29, 4534 (1984).

7 E. R. Weber and P. Omling, Festorper problems XXV, 623 (1992).